



Analytical-mechanical based framework for seismic overall fragility analysis of existing RC buildings in town compartments

Sergio Ruggieri¹ · Mirko Calò¹ · Angelo Cardellicchio² · Giuseppina Uva¹

Received: 27 December 2021 / Accepted: 6 September 2022 / Published online: 16 September 2022
© The Author(s) 2022

Abstract

The paper presents an analytical-mechanical based procedure to estimate the seismic overall fragility of existing reinforced concrete building portfolios in town compartments, as reduced areas of a municipality. The proposed methodology is based on two main concepts: (a) to consider all typological parameters characterizing the entire set of buildings located in a certain urban area and their variability through an analytical procedure; (b) to employ a mechanical approach by means of ideal numerical models to estimate the safety level of the focused sample of buildings. Hence, the methodology allows to compute seismic overall fragility curves, obtained by using laws of total variance and expectation and weighing factors proportional to the probability of having a certain configuration of typological parameters with determined values. To test the proposed procedure, some town compartments of the municipality of Bisceglie, Puglia, Southern Italy, were investigated by firstly identifying the most recurrent typological features exploiting multisource data, after by elaborating an extensive campaign of modelling and analysis on different ideal buildings (herein named realizations) and finally by computing fragility curves for each realization and for the set of ideal buildings. The results show overall fragilities curves for the investigated town compartments, which are obtained in a different way from the existing procedures, by avoiding an a-priori selection of one or more index buildings to represent the specific building portfolio and the definition of a specific building taxonomy.

Keywords Seismic overall fragility curve · Existing RC buildings · Typological parameters · Homogeneous town compartments

✉ Sergio Ruggieri
sergio.ruggieri@poliba.it

¹ DICATECH Department, Polytechnic University of Bari, Via Orabona, 4, Bari, Italy

² Institute for Intelligent Industrial Technologies and Systems for Advanced Manufacturing (STIIMA), National Research Council of Italy, Via Amendola, 122 D/O, Bari, Italy

1 Introduction

The study of the seismic behaviour of existing buildings in the areas characterized by medium–high seismicity is one of the topics faced in the recent years by the scientific community, which proposed several methodologies to predict the possible effects on the existing building stock at the occurrence of seismic events and to develop prioritization plans for destining available resources to seismic risk mitigation cause. The characterization of seismic risk depends on the hazard, the exposure and the vulnerability, where this latter is the factor that is usually object of reduction. The evaluation of the seismic vulnerability consists in the definition of a function that relates the seismic intensity to the damage state (or better, the possible losses), which is a concept requiring the performance of several steps. Especially for evaluating the seismic vulnerability (fragility when the losses are quantified through an engineering damage) of a set of buildings, several models can be employed, according to two main different categories, as well as empirical and mechanical methods (Silva et al. 2019). Several examples and applications are available in the scientific literature, where in the empirical methods the vulnerability functions are derived by relating observed damages to specific seismic events, while in mechanical methods the vulnerability functions are derived by relating specific analyses on numerical models representing one or a class of buildings. For both approaches, in the case of building portfolios investigation, the success of the analyses relies on two main dependences: (a) the accessibility and availability of input data; (b) the reliability of a building taxonomy to define a homogeneous class of buildings to investigate. Regarding to input data, besides the intensive investigations required in the case of single-building analysis, class-level studies are usually based on freely available databases and on the gathered information by local experts or technicians. These procedures of data collection become the input of the second aspect to manage in a large- (or urban-) scale vulnerability analysis, which is the definition of the taxonomy. This concept underlies a number of typological features that, if merged, represents the common denominator of several buildings showing the same overall seismic performance (with an adequate simplification). Both for the method to employ in the definition of the vulnerability/fragility function and for the input data and the related classification, a predominant component of subjectivity must be considered, which depends on several factors, such as the awareness and the formation of the analyst, the quality and quantity of data at disposal and the time for performing all necessary steps.

In this large range of possibilities and considering the existing sources of variability, this paper aims to provide an alternative method to evaluate the overall fragility for reduced urban areas, characterized by near-homogeneous buildings having recurrent features. In particular, the proposed approach answers to the following questions: can the current approaches for defining reliable vulnerability (or fragility) functions at class-level be improved in terms of objectivity? Can the same data and classification procedures provide the base for tracking trustworthiness risk mitigation plan in urban areas? Can few simplified archetype buildings or too many simplified models effectively reproduce the seismic performance of a class of buildings?

Obviously, these are still open issues, which are continuously object of scientific studies but the claim of this paper is to provide a solution to bypass some of the highlighted conventional approaches. Firstly, at the base of the proposed procedure, we developed an input database by exploiting the information obtained by different sources, e.g., census data, Technical Regional Cartography (CTR), the results of an interview-based approach and the features obtained by a labelling process on reinforced concrete (RC) buildings photos,

performed in Ruggieri et al. (2021a). Joining the different data sources, the proposed framework consists in a series of propaedeutic steps, aimed to compute seismic overall fragility curves for RC buildings in different urban areas (according to the CARTIS approach, urban areas are indicated as town compartments, TC). Namely, a statistical analysis of the typological parameters characterising buildings in the observed area is firstly carried out. Second, by combining all identified typological parameters, several ideal buildings (herein named realizations) are generated and analysed, by evaluating as output single fragility curves. Finally, the fragility curves of all realizations are combined to obtain an overall fragility curve for each TC, by using a weighted approach of the laws of total variance and total expectation. The weighing factors to adopt are evaluated on the base of the probability of having a certain configuration of typological parameters with determined values.

From this brief summary (the framework is extensively presented in Sect. 3), the advantages of the procedure can be immediately highlighted: (a) the procedure is applicable and scalable for different classes of buildings, made by different construction materials (herein the approach is developed for RC buildings); (b) the selection of index buildings and the definition of specific taxonomies are not strictly necessary; (c) the result of the procedure is one overall fragility curve for a TC and it is given by all recurrent typological parameters. On the other hand, the main disadvantage of the procedure is the possibility, in the case of typological parameters presenting high variability, to generate a very huge set of numerical models, which can be recovered for investigating other TCs constituted by buildings having the same involved typological parameters.

2 Background

The following Sections present the background and the more recent studies about input data to employ in vulnerability analysis (Sect. 2.1), the state of the art about methodologies for vulnerability analysis and the definition of seismic fragility with regard to single- and class-level applications (Sect. 2.2).

2.1 Evaluation of seismic fragility and vulnerability: input data, analysis approaches and observed area

The success of reliable seismic vulnerability/fragility analysis is strictly dependent on the availability and accurateness of input data, the type of analysis method and the area to investigate. Regarding to the input, in Polese et al. (2019) authors proposed a comprehensive list of sources from which extract data for vulnerability analysis: (i) Census data; (ii) interview-based methods; (iii) Geographic Information System (GIS) and remote sensing techniques; (iv) single-building analysis. Taking Italy as reference, several freely georeferenced databases can be accessed, such as the census databases, ISTAT (2011), containing the base information of buildings in an area (e.g., number of floors, construction material and year of construction), CTRs containing information on polygons of buildings located in an area (e.g., height, area), Cadastral maps containing contours of buildings. Using this information, a first vulnerability classification can be elaborated, even if the degree of accuracy is low and the seismic performance is usually estimated through vulnerability indexes (Indirli 2019; Zanazzi et al. 2019; Hansapinyo et al. 2020; Leggieri et al. 2022). A further and consistent improvement can be achieved through the integration of the above data with the results of interviews-based methods. To this scope, predefined survey forms

are elaborated, allowing to collect typological features for classifying buildings in a geographic zone. Namely, given an area to investigate, two techniques can be adopted: (i) an expert is questioned on the most recurrent features about the buildings occupying the territory and their evolution; (ii) a team of surveyors are commissioned to go into the area and to compile a questionnaire for each building. Always taking Italy as reference, the first option converges in the CARTIS procedure (Zuccaro et al. 2015), while the second option can be practiced through the GNDT approach (1993). For both types of procedures, although data are not yet fully accurate, a more refined information is obtained and seismic vulnerability functions can be developed by investigating the seismic performance of ideal buildings (or archetypes) identified on the base of an expert judgment (e.g., Donà et al. 2020; Brando et al. 2021; Vettore et al. 2020) or accounting for a parametrization made by range of input values (Leggieri et al. 2021). In addition, also post-earthquake damages data can be also considered as input of vulnerability analysis, especially for empirical methods. For example, all post-earthquake Italian data were recently collected in a catalogue elaborated by the Department of Civil Protection, named DA.D.O., Observed Damage Database (Dolce et al. 2019), and it was used within several recent papers proposing empirical vulnerability functions (Nicodemo et al. 2020; Del Gaudio et al. 2020; Ruggieri et al. 2021c).

With regard to vulnerability analysis methods, two methodologies are usually employed: empirical and mechanical methods (do not forgetting hybrid and rapid visual screening methods, e.g., Ruggieri et al. 2020a). Empirical methods consist in a statistical based processing of data, aimed to evaluate the probability of occurrence of a certain damage state for increasing seismic intensities. Vulnerability curves are obtained as output of the data processing, using an intensity measure (IM) that accounts for the expected losses. During the years, several papers were proposed about the topic, starting from the damage probability matrices by Braga et al. (1982), which defined a method to express the discrete probability that a certain damage, quantified according to a certain macro-seismic scale, occurs within a sample of damaged buildings. In Di Pasquale et al. (2005) authors developed a model for evaluating losses, using observed damages recorded after the earthquakes occurred in Italy. In Lagomarsino and Giovinazzi (2006) a method was proposed for identifying the vulnerability assessment of several building typologies in the Mediterranean area, relating macro-seismic and mechanical models on the base of post-earthquake observations. Recently, Del Gaudio et al. (2020) investigated the seismic vulnerability of the Italian building stock by using data of about 320.000 units from DA.D.O.. Similarly, Rosti et al. (2020) investigated the set of Italian unreinforced masonry buildings damaged by the seismic events occurred during the last 50 years. In addition, several works could be mentioned, with regard to specific buildings typologies, such as masonry churches (e.g., De Matteis et al. 2019; Morici et al. 2020; Ruggieri et al. 2020b). The alternative approaches to empirical methods (and perhaps the most adopted ones) are the mechanical methods. Especially for classes of buildings, the reliability of the vulnerability function developed through mechanical methods depends on the kind of modelling approach and the type of analysis (Silva et al. 2019). Obviously, the more complex are the mechanical models and the more detailed are the analyses to perform, the greater the effort required. For this reason, mechanical models are always comprised between the two modelling extremes, which are the single-degree-of-freedom (SDOF) and the multi-degree-of-freedom (MDOF) approaches. Several examples of mechanical models developed through SDOF approach were proposed by scientific literature, such as the method by Borzi et al. (2008) that provided a simplified method named SP-BELA for the analysis of existing RC buildings. In Silva et al. (2014) authors investigated the vulnerability model of Portuguese RC buildings through a SDOF modelling approach, as well as made by Villar-Vega et al. (2017)

for the residential buildings in South America. In Kohrangi et al. (2021) authors adopted the paradigm of the Performance Based Design through the Yielding Frequency Spectra approach, to develop the vulnerability model of Isfahan, Iran. Alternatively, examples of MDOF approaches are available. In Del Gaudio et al. (2015) authors proposed a method to perform the fragility assessment of an urban area, by employing nonlinear static analysis on simplified shear-type structural model. In Aiello et al. (2017) authors performed the vulnerability assessment of the municipality of Bovino, Southern Italy, by means of an automated approach that varied the properties of four index buildings. Recently, analytical-mechanical methods were used for evaluating seismic fragility curves of different building typologies according to the damages observed after earthquake events. Polese et al. (2015) proposed a hybrid method to derive fragility curves by combining observational empirical data and buildings' residual capacity obtained by mechanical assessment. Del Gaudio et al. (2017) investigated urban seismic fragility for a sample of 250 buildings subjected to the L'Aquila Earthquake, comparing results of a simplified mechanical method and damages obtained from post-earthquake emergency survey. Later, Del Gaudio et al. (2018) used a simplified mechanical method for deriving damage scenarios for an enlarged database of RC buildings subjected to the 2009 L'Aquila earthquake and evaluated results according to damage classification by EMS-98. Riga et al. (2017) performed seismic risk assessment at urban scale by employing the method of Capacity Spectrum, by applying this approach on the city of Thessaloniki. Smerzini and Pitilakis (2018) proposed a tool for the seismic risk assessment at urban scale, by simulating earthquake ground motions effect through an accurate 3D-physics simulation. Recently, Zucconi et al. (2022) presented a method to estimate fragility curves of RC frame building classes, by using data from the 2012 Emilia and the 2009 L'Aquila earthquakes. Borzi et al. (2021) compared simulated and observed damage scenarios, according to the damages of the European Macroseismic Scale. A comprehensive state of the art of the main recent applications in the Italian scenario is reported in da Porto et al. (2021).

In the end, focusing on the area to investigate, a key role in the vulnerability function definition is played by the size of the area itself. As a matter of fact, a larger area implies different kinds of buildings, which present different behaviours and cannot be homogenized under a class. For this reason, the seismic vulnerability of larger areas is evaluated on set of buildings that present few similar features (e.g., construction typology, number of storeys). This introduces the concept of building taxonomy, and the recent literature proposes several examples elaborated on the building stock of a Country or of a Region. Some fairly popular taxonomies are the Medvedev-Sponheuer-Karnik scale, MSK-64 (Medvedev et al. 1965), the European Macroseismic Scale, EMS98 (Grünthal 1998), Hazus (1999). Other examples of more recent building taxonomies are the one defined within the RISK-UE projects (Mouroux et al. 2004), where a matrix of 23 building typologies was developed, according to seismic performance of the most recurrent European buildings, and the GEM Building Taxonomy (Brzev et al. 2013), which was based on a framework that account for the seismic performance of several buildings characterized by different construction typologies.

2.2 Seismic fragility analysis: a brief overview and applications from single-to class-level

The seismic fragility is an efficient way to quantify the predisposition of a building or a part of it to damage under seismic actions. The general idea underlying the definition of

a fragility curve is to provide a reliable measure of the safety (i.e., when talking about ultimate limit-states) than the result obtained by a deterministic approach. In this latter, as adopted by the European and Italian building codes (Eurocode 8 1998; NTC 2018), a safety factor is defined toward a limit-state of interest and a single number is determined to represent the ratio between seismic demand and structural capacity, usually defined via pushover analysis. Although from a practical point of view a safety factor represents the simpler way to quantify fragility, it does not consider the high variability of several aspects characterizing demand and capacity, which are known under the name of uncertainties. In general, sources of uncertainties are related to both capacity and demand quantities and they can be categorized under two different typologies, as defined by Der Kiureghian and Ditlevsen (2008): (1) aleatory; (2) epistemic. Especially in the case of existing buildings, each of the above categories implies other subsets of uncertainty sources, which could be distinguished as proposed by Bakalis and Vamvatsikos (2018) or that can be simply summarized as follows:

1. Uncertainty in the seismic demand, identified through the record-to-record variability, given by the ground motion arbitrariness and the selection of the IM (Kazantzi and Vamvatsikos 2015; O'Reilly 2021);
2. Uncertainty in the structural capacity, related to the kind of numerical model employed in the analysis (Zeris et al. 2007; Lachanas and Vamvatsikos 2021), to the knowledge of all involved geometrical and mechanical parameters (Vamvatsikos and Fragiadakis 2010) and to the definition of the limit-state (Liel et al. 2011; Galanis et al. 2015);
3. Uncertainty in the interaction between demand and capacity, given by the employed method of analysis (Fragiadakis et al. 2014) and the relation to establish between the IM and the engineering demand parameter (EDP).

The general definition of seismic fragility is the evaluation of the probability that the seismic demand exceeds or violates the structural capacity at the variation of the seismic intensity level and for a certain limit-state. From the mathematic point of view the seismic fragility is quantified through a fragility curve, which is a cumulative distribution function that expresses the probability of exceeding a predefined limit-state (according to an EDP threshold value defined under a certain criterion), given a value of the IM. It can be expressed as:

$$F(IM) = P(\text{Limit state exceeded} | IM) = P(EDP_D > EDP_C | IM) = P(IM > IM_C) \quad (1)$$

where C and D are, respectively, the capacity and the demand. As shown in Eq. 1, the fragility curve is a function F of the IM, usually defined to be efficient for the structure under investigation, in order to reduce the record-to-record variability and to be sufficient, in order to limit the dependence of the analysis results from seismological parameters. Still, the two right terms of Eq. 1 indicate the comparison between D and C and, at the same time, reveal the close relationship of the selected IM and EDP. As a matter of fact, for accounting uncertainty and for characterizing the evolution of the relation between EDP and IM, multiple nonlinear dynamic analyses are necessary, such as incremental dynamic analyses (Vamvatsikos and Cornell 2002), multi-stripe analyses (Jalayer and Cornell 2009) or cloud analyses (Miano et al. 2018; Nettis et al. 2021). Using these analysis methods, it is possible to characterize the EDP-IM space, in which evaluate the distribution (or probability density function) of one parameter compared to the other. Once the probability density function is known, the fragility curve can be obtained by fitting all the discrete

probabilities of exceeding one parameter, given the other (once the EDP threshold of the limit-state is fixed). Considering that a lognormal distribution is usually assumed for the IM-EDP relationship, the parameters characterizing a fragility curve are the median (generally expressed with μ) and the dispersion (generally expressed with β), both directly estimated by elaborating 16%, 50% and 84% fractiles of IM, by opting for moment method or by employing the maximum likelihood approach (Baker 2015).

The concept of fragility curve can be also applied to a sample of buildings (class-level), with the aim to represent the seismic fragility of a homogenous class of structures or, in some cases, to evaluate a single building fragility on the base of the fragility of its components (e.g., Nielson and DesRoches 2007). Regarding to analytical procedures, one of the first approaches was provided by Shinozuka et al. (2000), which evaluated class fragility curve for two bridges, starting from the statistical parameters of the single fragility curves. In Ruggieri et al. (2021b) authors adopted an analytical approach for computing class fragility of a sample of 15 school buildings, by elaborating fragility curves obtained on each building of the sample and by employing the laws of total variance and total expectation. This application allows to take into account (in addition to the record-to-record variability), intra-building and inter-building variabilities, as occurs when class fragility is considered. Intra-building variability is related to the uncertainty given by the building analysed and its properties (e.g., mechanical and geometrical features, numerical model). Inter-building variability is related to the presence of different buildings to represent the same class and the different responses to the same records employed in the analysis. As reported in Silva et al. (2019), inter-building uncertainty dominates the intra-building one, because it is expected high variability related to the class fragility obtained by different buildings belonging to the same class.

From the formal point view, assuming that the parameters of a class fragility curve are the class median (μ_{class}) and dispersion (β_{class}), the natural logarithm of the μ_{class} is estimated as the mean of the natural logarithm of all individual medians (μ_y) of single building fragility curves (considering N the total number of involved buildings), while β_{class} is provided by the square-root-of-sum-of-square of intra-building (β_{intra}) and inter-building (β_{inter}) variabilities. The first one aims to evaluate the differences in median response of all buildings and can be computed as the standard deviation of the medians, or the second order moment, while the second term can be evaluated through the mean of the individual fragility curves dispersions, β_y , or first order moment:

$$\ln \mu_{class} = \frac{1}{N} \sum_{y=1}^N \ln \mu_y \tag{2}$$

$$\beta_{class} = \sqrt{\beta_{intra}^2 + \beta_{inter}^2} \tag{3}$$

$$\beta_{intra} = \sqrt{\frac{\sum_{y=1}^N \beta_y^2}{N}} \tag{4}$$

$$\beta_{inter} = \sqrt{\frac{\sum_{y=1}^N [\ln \mu_y - \ln \mu_{class}]^2}{N}} \tag{5}$$

The methodology adopted in this paper is based on Eqs. 1–5 and it will be explained in detail in Sect. 3. It is worth mentioning that the above expressions, obtained from laws of total expectation and total variance, are always valid despite the typology of distribution. As also mentioned in Bakalis and Vamvatsikos (2018), in some cases (e.g., large dispersion of the structural capacity) the overall fragility could be not effectively lognormal.

3 Weighted seismic overall fragility: proposal of an analytical-mechanical based framework

The approach proposed in this paper aims to evaluate a weighted seismic overall fragility for RC buildings in a TC, based on an analytical-mechanical framework, as shown in Fig. 1. The framework is elaborated and released for RC buildings, but it can be easily extended to other building typologies (e.g., masonry, steel). The procedure, following described, is subdivided in 6 steps.

3.1 Step 1: input data from different sources

The first step consists in the data collection about the zones under investigation. This phase is developed on the base of the means at disposal by the analyst. In our proposal, we exploit several data sources, accurately choosing which ones must be fused. As shown in the first box of Fig. 1, the exploited sources are:

- Census database, which in the Italian case is represented by the ISTAT database (2011). It contains, for each Census section, the year of construction of all buildings belonging to an area, the percentage of buildings having a specific construction typology, the state of maintenance and indications about the number of storeys.

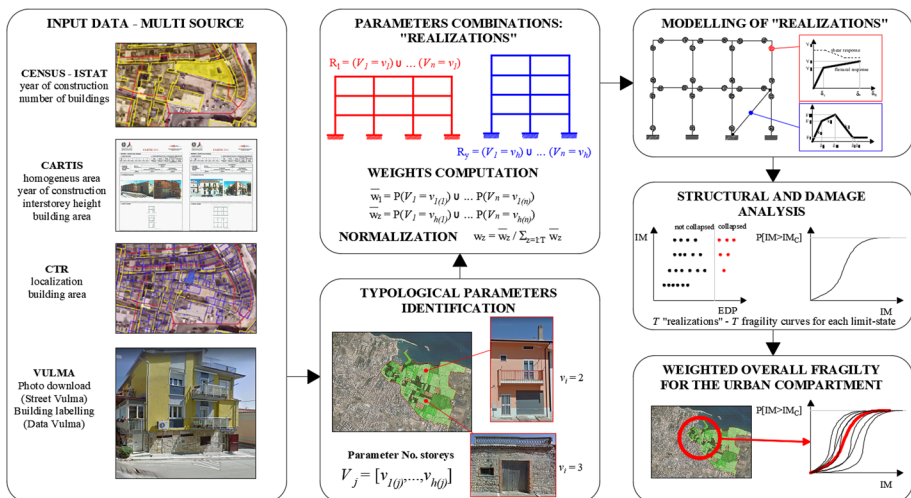


Fig. 1 Flow chart of the proposed analytical-mechanical approach

- CARTIS database, which is the final database of the CARTIS procedure application. This database, available where the procedure has been effectively applied, contains for each building information about construction typology, year of construction, interstorey height, base area, foundation type, presence or not of non-structural elements, number of windows per storey. In addition, the main advantage of CARTIS is that allows to identify homogeneous areas containing buildings having similar features and then, to properly identify the TCs of a municipality;
- CTR, which contains georeferenced polygons containing information about the enclosed buildings, such as the use destination, buildings area and height;

To these data, which cover the most useful information for an urban-scale study, we propose to use an additional tool, recently developed and named VULMA (Ruggieri et al. 2021a), which is a machine-learning framework for evaluating the vulnerability analysis of an existing building starting from a photo. Briefly, VULMA is characterized by four modules: (1) Street VULMA, which processes raw data to extract photos of buildings from an area; (2) Data VULMA, which allows domain expert to store photos of buildings once that they have been labelled; (3) Bi VULMA, which is composed by a set of machine-learning algorithms (based on convolution neural networks) that, once trained, are able to capture the labelled features of buildings and (4) In VULMA, which provides a simple vulnerability index for a single building. For our scopes, the first two modules are the necessary ones, where the photos of an area under investigation are downloaded (Street VULMA) and each photo is labelled according to some typological features (Data VULMA). Labels assigned to the photo usually are: number of storeys, presence of pilotis floor, presence of superlevation or basement floor, type of roof floor, presence of higher ground floor, presence of overhangs and possible irregularity (in-plan or in-height).

The use of all abovementioned data provides a near-full knowledge about the typological features of the building stock in the area under investigation, and data represent the input of the next step. Obviously, the disposition of all data is not always possible and, for this reason and to generalize the Step 1, the minimum requirements for the procedure are represented by the year of construction, the construction typology, the base area, the number of storeys and the building height. In this way, the mechanical models (see Sect. 3.4) will be extremely simplified, such as SDOF models as adopted in Khorangi et al. (2021) or in Ruggieri and Uva (2021). To have more data implies to have a better prediction of the TC seismic fragility because the mechanical models to generate can be more elaborated and will return more reliable results. In addition, if two different sources provide a different value of the same datum, the right one is provided by the more detailed and recent source (e.g., CARTIS or VULMA).

3.2 Step 2: typological parameters identification

Once the information on buildings enclosed in the area under investigation is available, the second step consists in the identification of all useful typological parameters, along with their related values. As a matter of fact, the entire building stock in a TC should be characterized by the same period of construction and typological features, and this usually drives the analyst to select only one or few index buildings to represent this area. Nevertheless, more than one building could present different typological features, e.g., renovations or demolition and reconstruction actions, evidence that an approach based on index buildings cannot take into account. Then, in the proposed procedure, all typological parameters are

characterized by all the possible values actually observed. From the mathematical point of view, let us suppose that a total of n typological parameters, V_j , can be identified:

$$V_j, j \in [1, \dots, n] \quad (6)$$

Each V_j can be characterized by a set of observed values, v_i , where i can assume a maximum value, generically indicated with m . The number m can assume different values on the base of the considered parameter V_j :

$$V_j = [v_1, \dots, v_m], i \in [1, \dots, m] \quad (7)$$

Larger values of m imply a large set of values v_i characterizing the parameter V_j , which lead to an exponential grow of the typological classification and quickly making the problem untreatable. Hence, the number of observed values can be reduced by using a data binning approach, aimed to smartly reduce the number m of allowed values to a number h , where $h < m$. To define h , values v_i must be grouped according to a certain beginning criterion, Φ , which can be either qualitative or quantitative. For example, if V_j represents the typological parameter *number of storeys*, the observed values (e.g., 1, 2 and 3) can be grouped into the new parameter *low-rise*, by provoking the transition from m to h . Furthermore, bins size may not be uniform, but it can be selected according to domain-related considerations. The selection of Φ is obviously domain-related and depends on the specific interpretation of V_j . As for the previous example, Φ can be selected considering well-known practices in urban-scale seismic analysis, but we must note that this simplification implies the definition of a taxonomy. However, it is important to underline that this assumption simplifies the next steps of the proposed method and, at the same time, does not force the analyst to follow an imposed typological classification. Other simplifications are herein proposed:

- Year of construction: buildings are divided according to their period and the related building code. Specifically, three periods are identified: (1) absence of seismic code provisions; (2) low detailed seismic code provisions and design with admissible stresses; (3) full detailed seismic code provisions and design with limit-states.
- Base area: buildings are divided according to their base area, where the thresholds are assumed to 200 m² and 400 m² i.e., buildings whose area is above, comprised and below the suggested thresholds.
- Number of openings per floor: buildings are divided by using a thresholds value of 3 and 5 openings per floor. In this case the CARTIS approach that relies on the absolute percentage of openings is not used.

On the base of the input data, a set of V_{j^*} typological parameters has been considered, with:

$$j^* \in [1, \dots, 13] \quad (8)$$

These parameters, along with the related binning criterion, are reported in Table 1. In this latter, each observed set of values can assume three kinds of assignments: (1) a number, integer or not, depending on the type of parameter; (2) a typological indication, as well as occurs for a significant detail of the building; (3) a Boolean value (that is, *true* or *false*), related to the presence of a certain element. Considering that each V_{j^*} accounts for a different quantity of values, two formal assumptions are supposed: (i) $h(j^*)$ indicates the number

Table 1 Typological parameters identification (V_{j^*}), kind of assignment (number, typology and Boolean) of v_i and adopted source (the item “construction material” is not inserted, because the procedure is referred to RC buildings)

Typological parameter (V_{j^*})	Kind of assignment	Discretization (v_i)	Sources
Year of construction (V_1)	Number	1980 (v_1) 1980–2008 (v_2) > 2008 (v_3)	ISTAT, CARTIS
Number of storeys (V_2)	Number	Low-rise (v_1) Mid-rise (v_2) High-rise (v_3)	ISTAT, CARTIS, VULMA
Base area (V_3)	Number	< = 200 m ² (v_1) > 200 m ² ; < = 400 m ² (v_2) > 400 m ² (v_3)	CTR, CARTIS
Presence of masonry infills (V_4)	Boolean	Yes (v_1) No (v_2)	VULMA, CARTIS
Presence of pilotis floor (V_5)	Boolean	Yes (v_1) No (v_2)	VULMA, CARTIS
Presence of basement floor (V_6)	Boolean	Yes (v_1) No (v_2)	VULMA, CARTIS
Presence of higher ground floor (V_7)	Boolean	Yes (v_1) No (v_2)	VULMA, CARTIS
Presence of superelevation floor (V_8)	Boolean	Yes (v_1) No (v_2)	VULMA, CARTIS
Number of openings per floor (V_9)	Number	< = 3 (v_1) > 3; < = 5 (v_2) > 5 (v_3)	VULMA
Type of roof floor (V_{10})	Typology	Flat (v_1) Pitched (v_2)	VULMA, CARTIS
Presence of overhangs (V_{11})	Boolean	Yes (v_1) No (v_2)	VULMA, CARTIS
Regularity in-plan (V_{12})	Boolean	Yes (v_1) No (v_2)	VULMA, CARTIS
Regularity in-height (V_{13})	Boolean	Yes (v_1) No (v_2)	VULMA, CARTIS

of values h for each parameter j^* ; (ii) the vector of values for each V_{j^*} is indicated as $[v_{1(j^*)}, \dots, v_{h(j^*)}]$.

3.3 Step 3: parameters combination, weights computation and normalization

Given the parameters V_{j^*} with the related values $[v_{1(j^*)}, \dots, v_{h(j^*)}]$, the third step of the proposed approach combines all V_{j^*} , which were assumed to be independent variables. Supposing that an ideal building having a specific $v_{i(j^*)}$ for each V_{j^*} , the set of typological parameters $v_{i(j^*)}$ identifying the structure is \mathbb{V} . Assuming then a generical value $v_{i(j^*)}$ for a set of V_{j^*} , \mathbb{V} can be mathematically defined as:

$$\mathbb{V} = \{v_{i(1)}, v_{i(2)}, v_{i(3)}, \dots, v_{i(13)}\}, i \in [1, \dots, h] \tag{9}$$

The ensemble \mathbb{V} characterizes an ideal “realization” denoted as R_y . This latter is not a real or an index building, as it is not guaranteed that R_y is contained in the building stock of the area under investigation. Instead, R_y is an ideal structure, representative of the given typological features within the entire set of observed buildings in the observed area. To quantify the number of possible realizations that can be produced by the combination of the typological parameters, we use the symbol T , where:

$$y \in [1, \dots, T] \tag{10}$$

and each of the n parameters V_{j^*} can assume at most the h possible values $v_{i(j^*)}$. Obviously, this is a simplifying assumption as, ideally, each parameter can assume an arbitrary number of values. However, this hypothesis leads to obtain a simplified and generalized representation of the total number of possible realizations T for the n parameters, that is:

$$T = \prod_{j^*=1}^n \Psi(V_{j^*}) \tag{11}$$

where Ψ is a function indicating the cardinality of the vector of values $v_{i(j^*)}$ characterizing each V_j . Each ideal building or realization can be numerically generated, analysed and all obtained results are used to evaluate the overall seismic fragility of the buildings in the focused TCs (as shown in the next Sections).

On the other hand, it is worth paying attention to the role of each realization in the overall fragility, considering that ideal buildings are characterized by parameters having different probability of occurrence in the areas. This means that each realization assumes a different weight in the overall fragility of each TC and then, it is necessary to evaluate a specific weight for each realization within each TC. To this scope, the law of total probability can be employed to evaluate the compound probability of all involved typological parameters and the related values of all realizations in the observed areas. Assuming that the generic weight is \overline{w}_z , it can be computed as follows:

$$\begin{aligned} \overline{w}_z &= P(V_1 = v_{i(1), \dots, h(1)} \cup V_2 = v_{i(2), \dots, h(2)} \cup \dots \cup V_n = v_{i(n), \dots, h(n)}) \\ &= P(V_1 = v_{i(1), \dots, h(1)}) \cdot P(V_2 = v_{i(2), \dots, h(2)}) \cdot \dots \cdot P(V_n = v_{i(n), \dots, h(n)}) \end{aligned} \tag{12}$$

where $P(V_{j^*} = v_{i(j^*), \dots, h(j^*)})$ is the probability that V_{j^*} assumes the value $v_{i(j^*), \dots, h(j^*)}$ and z is contained in the same domain of y . The weights as well as computed should be normalized as in Eq. 13, to obtain a unitary sum of all weights (Eq. 14), where the total number is T :

$$w_z = \frac{\overline{w}_z}{\sum_{z=1}^T \overline{w}_z} \tag{13}$$

$$\sum_{z=1}^T w_z = 1 \tag{14}$$

Considering that some parameters do not present a numerical value, the statistical quantification can be expressed in percentage terms, by counting the number of buildings having a certain $v_{i(j^*)}$ for a certain V_{j^*} on the total buildings having that V_{j^*} and belonging to the observed area and after applying the law of total probability. The generic normalized

weight, w_z , can assume a value ranging from 0 to 1 and its value depends on the probability that V_{j^*} assumes a value $v_{i(j^*)}$ in all observed buildings in the area under investigation. In particular, in the buildings of the entire area the following occurrences can be denoted:

- $P(V_{j^*}=v_{i(j^*)})=1$, which implies that all observed buildings present a fixed value v_i for the parameter V_{j^*} and it is always valid (it can be excluded from the combination);
- $P(V_{j^*}=v_{i(j^*)})=0$, which implies that none of the observed buildings present the value v_i for the parameter V_{j^*} and it is never valid (it provides $\overline{w_z}$ equal to 0);
- $0 < P(V_{j^*}=v_{i(j^*)}) < 1$, which implies that some buildings present the value $v_{i(j^*)}$ for the parameter V_j and other buildings present a different value $v_{i(j^*)}$ for the parameter V_{j^*} (it contributes to obtain the weight $\overline{w_z}$);

At this point, all the w_z can be put aside for the moment (they will be resumed in the Sect. 3.6) and all realizations can be investigated separately and as if they are equiprobable and representative of the real buildings in the area under investigation.

3.4 Step 4: modelling of realizations

For each realization a numerical model can be generated. To this scope, considering that the realizations are ideal buildings, a process of simulate design can be employed, according to the prescriptions provided by the current building code in the focused period of construction. In particular, observing the proposed discretization in Table 1 and looking at the Italian case, admissible stresses or limit-states methods can be used, according to absent, low or full seismic detailed indications provided by the different releases of building codes. In addition, the procedure of simulate design is necessary to establish loads, materials and geometry, where this latter regards the number of bays in both main directions and the sizes of columns and beams. This process is strictly related to the analyst's experience, which has the task to avoid unreal situations and to faithfully reproduce the constructive practice of the identified period of construction. Once the missing structural parameters have been designed, the realizations can be numerically modelled. Three-dimensional models are strongly suggested (simplified or bidimensional models could represent an additional simplification that can be avoided), while the nonlinear modelling approach and the structural software to use can be selected by the analyst. For the case at hand (see Fig. 1) the simpler approaches can be employed for nonlinear modelling, as using plastic hinges according to the prescriptions provided by the current Italian building code (NTC 2018) and involving the nonlinear macro-element with in-plane behaviour proposed by Panagiotakos and Fardis (1996) for masonry infills. Nevertheless, several improvements can be obtained by opting for more refined methodologies. For example, plastic hinges formulation can be improved according to recent developments in O'Reilly and Sullivan (2018), while masonry infills can follow the recent achievements by Verderame et al. (2022) and Di Trapani et al. (2021). If T is a high number, the phase of simulation and modelling of the ideal building can represent a hurdle in a view of time and computational efforts. On the other hand, a realization used for investigating the fragility of a TC can be recycled for investigating the fragility of another TC. The unique difference between the two areas of the municipality is the weight assumed by each realization in the TC, given by the different frequency of occurrence of the typological parameters characterizing the model. Hence, the same realization has a different value of w_z in two different TCs. Still, the generation

of several realizations leads to have a twofold advantage with regard to an index building approach: (a) there is no any possibility to fail in the “right” selection of the index buildings, which is necessary to accurately define an overall fragility; (b) the generation of T realizations allows to reduce the building-to-building variability (or inter-building variability) given by the selection of few index buildings, which is usually the most significant in class fragility analysis if compared to the intra-building variability.

3.5 Step 5: structural and damage analysis

When each realization is modelled, structural and damage analysis can be performed. Regarding to the structural analysis, each numerical model is investigated through non-linear dynamic analyses and, to this scope, any methodology can be employed, such as cloud, multi stripe or incremental dynamic analyses, on the base of the analyst’s preference. About this topic some aspects need to be clarified. First of all, being an urban scale analysis, the records selection shall follow as convenient criterion as possible, which joins the necessity to represent the seismic hazard of an area and to use an IM representative of different numerical models within an entire class. To this twofold aim, in the proposed procedure we suggest to follow the approach proposed by (Kohrangi and Vamvatsikos 2016), as extension of the conditional spectrum approach (Lin et al. 2013; Khorangi et al. 2017). In this latter, researchers performed a record selection for different European cities, in order to obtain two sets of ground motion records for moderate- and high-seismicity sites. That selection was made by adopting as IM, the average spectral acceleration ($AvgSa$) for a large set of periods, as well as for a range going from 0.3 to 3 s and for a mean annual frequency of 2% in 50 years. To be more accurate, record selection can be processed by employing information from microzonation of the observed area, where available, exploiting the possibility to account for effects that are usually neglected at this scale of analysis, e.g., soil amplification (this aspect is discussed later, in Sect. 4.3). After, regarding to the number of records to employ, the choice depends on several factors, such as the type of structure, the type of IM, the type of EDP and the dispersion of the EDP given the IM. Obviously, using more ground motions records has the advantage to reduce the record-to-record variability but, at the same time, the disadvantage of increasing the time of analysis. As rule of thumb, we suggest to employ at least 11 ground motion records with two horizontal components as in (Ruggieri et al. 2021b), even if in the application of the proposed procedure (see Sect. 4), 30 ground motion records with two horizontal components were used. Finally, regarding to the EDP, also in this case the selection depends on the analyst’s choice. Nevertheless, another aspect to take into account is the limit-state to investigate. As a matter of fact, for ultimate limit-states, a typical EDP is the maximum interstorey drift ratio (θ_{max}) but for serviceability limit-states other EDPs can be selected, such as the peak floor acceleration. In this work, only the safety limit-states will be accounted for (ductile and brittle mechanisms) and the selected and suggested EDP is the θ_{max} . Regarding to the damage analysis, fragility curves can be estimated, by evaluating the conditional probability of exceeding of EDP to a certain capacity threshold, which is related to a damage that, if exceeded, provides the transition to another damage state. The computation of the fragility curves, as just mentioned in Sect. 2.2, must be performed for each realization, obtaining a number T of fragility curves for each limit-state of interest, each one characterized by proper μ_i and β_i .

3.6 Step 6: weighted overall fragility for town compartments

The obtained results in terms of fragility curves can be used to compute the overall seismic fragility for the limit-states of interest, according to Eqs. 2–5. Nevertheless, the structural and damage response of each realization assumes a different importance within the observed areas, because the input typological features are differently distributed and then, the realizations are not considerable as equiprobable. For this reason, the weights computed in Sect. 3.3 can be resumed and used to weigh the overall fragility of the TCs. In particular, by matching the laws of total expectation and total variance and the results of the compound probability of the input parameters and the related values, the ensemble lognormal mean is given by the weighted mean of all individual lognormal means, μ_y , and Eq. 2 can be re-edited as follows:

$$\ln\mu_{\text{overall}} = \frac{\sum_{y,z=1}^T w_z \cdot \ln\mu_y}{\sum_{z=1}^T w_z} \tag{15}$$

where the term N of Eq. 2 is now indicated as T . Still, with regard to dispersions, β_{intra}^2 is provided by the weighted mean of the individual fragility curves variabilities, β_y^2 , while β_{inter}^2 is computed as the weighted standard deviation of the individual median values, μ_y . Hence, Eqs. 4 and 5 can be re-edited as follows:

$$\beta_{\text{intra}}^2 = \frac{\sum_{y,z=1}^T w_z \cdot \beta_y^2}{\sum_{z=1}^T w_z} \tag{16}$$

$$\beta_{\text{inter}}^2 = \frac{\sum_{y,z=1}^T w_z \cdot [\ln\mu_y - \ln\mu_{\text{overall}}]^2}{\frac{M-1}{M} \cdot \sum_{z=1}^T w_z} \tag{17}$$

where M is the number of non-zero weights and μ_{class} and β_{class} have been changed in μ_{overall} and β_{overall} . From the mathematical point of view, the weighing procedures for the first and second order moments are admissible. From the physical point of view, two aspects should be denoted. Firstly, weighing the standard deviation implies a variation of the obtained damage distributions of each realization. In addition, the proposed computation of the weighted overall fragility can lead to have not a real lognormal distribution, but only a curve having an S shape. On the other hand, it is worth remembering that also by considering all buildings as equiprobable in the ensemble (Eqs. 2–5), the resulting overall fragility curves could have not a lognormal distribution, as restated in Bakalis and Vamvatsikos (2018) and in Shinozuka et al. (2000). Still, the modification of the damage distribution (and implicitly of the EDPIIM distribution) can be taken into consideration, by thinking that the realizations are not real or index buildings but they are only the simulated means to represent all the observed typological features in the existing building stock. In the end, it is possible to briefly summarize the pros and cons of the proposed procedure:

- As advantages, the proposed procedure does not strictly depend on a building taxonomy, as well as does not require the definition or the selection of right index buildings. All realizations, as proposed, take into account all main typological parameters that are included in an urban-scale fragility analysis. Parameters are adequately weighted for obtaining a reliable result. Still, given a municipality with different TCs, if they are

characterized by buildings with similar features, the models and analyses used for one TC can be extended to other TCs;

- As disadvantages, the proposed procedure needs of several information sources for accurately determining the input typological parameters (e.g., VULMA) and the generation and analysis of the realizations can be a long and time-consuming process. For these reasons, the procedure is strongly suggested for not extended areas, as for the TCs having homogeneous typological features (as defined in CARTIS).

4 Case study: some town compartments of the municipality of Bisceglie, Puglia, Southern Italy

The proposed procedure was applied on the case study of the municipality of Bisceglie, Puglia, Southern Italy. As shown in Fig. 2, Bisceglie is located in the middle of the Region, which presents a growing seismicity from the South to the North, with values of the peak ground acceleration (PGA) comprised between 0.025 and 0.25 g (where g is the gravity acceleration). For the observed area, a medium seismicity is recorded, with values of PGA ranging from 0.10 and 0.20 g accounting for a probability of exceeding of 10% in a reference period of 50 years and soil category of type A (PGA values that can increase for different soil and topography categories). The municipality overall presents a building stock homogeneously distributed between RC and masonry units, as well as an historical centre and several expansion zones realized during the years. In addition, the closest part to the

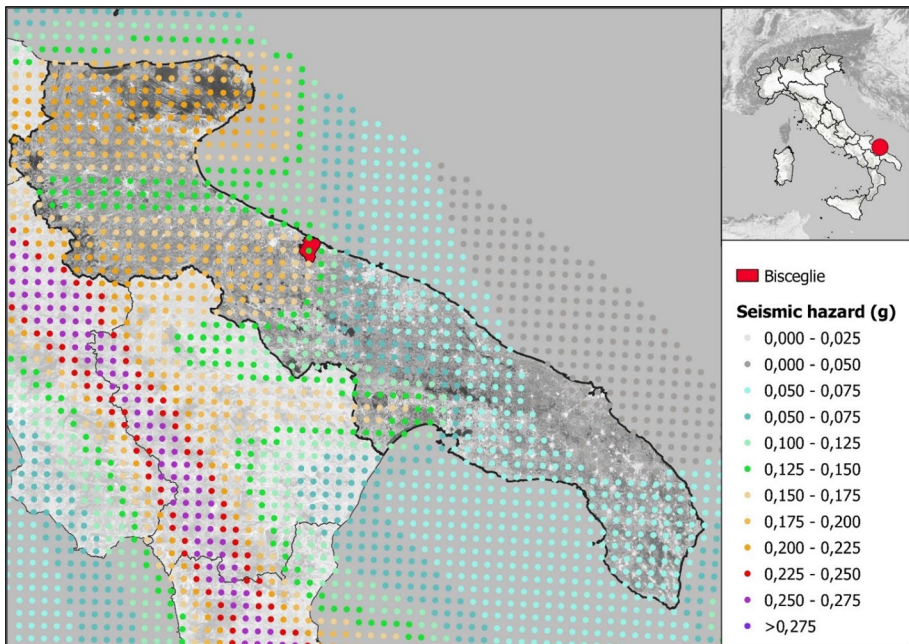


Fig. 2 Seismic hazard map of Puglia Region, with indication of the municipality of Bisceglie and the PGA distribution for a probability of exceeding of 10% in a reference period of 50 years and soil category of type A

sea is characterized by buildings while the rest of the territory is a rural zone. A more comprehensive description of the different areas of the municipality and the input data, necessary to apply the proposed procedure, is reported in Sect. 4.1.

4.1 Input data, definition of the most recurrent typological features and weights computation

The first screening of the building stock of Bisceglie is made by means of the ISTAT database (2011), where the total amount of residential buildings is approximately equal to 4200, subdivided among 31% of masonry, 63% of RC and 6% of other materials. In addition, the 62% of the units were built before the 1980, the 34% between the 1980 and the 2008 and the 4% after the 2008. After, the CARTIS procedure is available for the municipality and, in particular, Bisceglie is subdivided in 8 TCs, each one characterized by similar typological classes of masonry buildings (indicated with MUR) and RC buildings (indicated with CAR). All the TCs are shown in Fig. 3 and they are tagged as C01-C08. C01 is the historical centre of Bisceglie, near fully characterized by masonry buildings and presenting a minority of RC buildings. C02 and C03 are the first and second expansion zones, respectively, constituted by a quasi-equal distribution of masonry and RC units. C04, C05, C06 and C07 are the third and fourth expansion zones (from 1950) and they extend around the previous TCs and contain the most of the entire building stock. Finally, C08 is the touristic expansion zone, prevalently constituted by new RC buildings. The percentage distribution of buildings in the TCs is provided in Fig. 4, accounting for construction material (left) and number of units per TC (right).

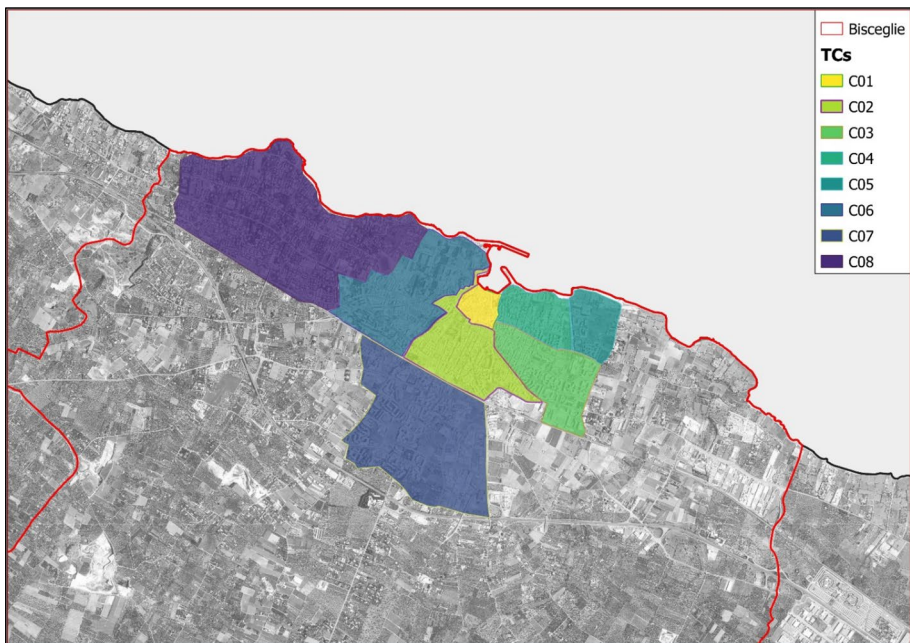


Fig. 3 TCs for the municipality of Bisceglie (according to CARTIS procedure)

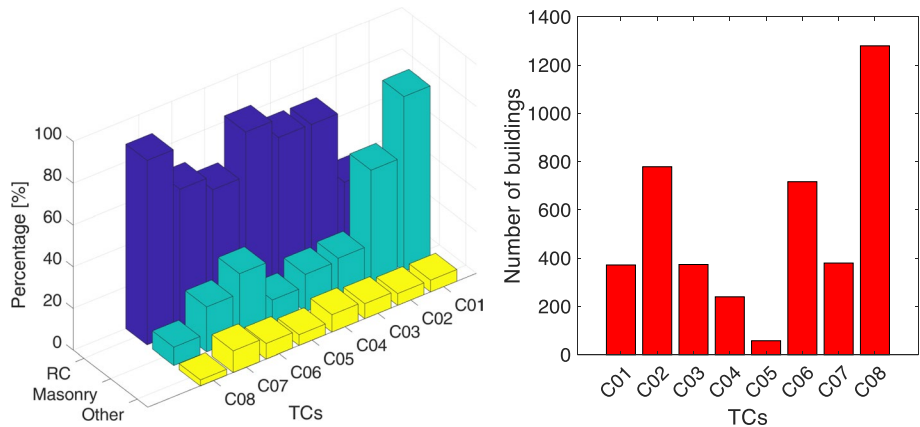


Fig. 4 Percentage distribution of buildings for the construction material parameter (left); number of units per TC (right)

In order to apply the proposed procedure 5 TCs were selected: C01, C02, C03, C04 and C05. The selection of these five areas is not casual and it resides in some preliminary considerations by authors. From the geographic point of view, the TCs extend to the East and they contain the older buildings of the municipality, both in masonry and RC. In addition, about these areas we dispose the photos of all buildings as reported in Ruggieri et al. (2021a), where each photo was labelled according to the typological parameters indicated in Table 1. Figures 5 and 6 report the maps about the Census sections and the CTR, respectively, juxtaposed on TCs and providing useful data (as reported in Sect. 3.2). Figure 7 reports a couple of labelled photos of RC buildings taken through VULMA from C04 (left) and C05 (right). Having at disposal all data, steps 2 and 3 of the proposed procedure can be performed. In particular, for all RC buildings of the 5 TCs, the typological parameters in Table 1 were defined and, for each TC, Eq. 12 was applied, having as output the frequency of occurrence of the values $v_{i(j^*)}$ for each typological parameter V_{j^*} . Table 2 reports, besides the total number of RC buildings in each TC, the frequency of occurrence in percentage terms of all $v_{i(j^*)}$ for each V_{j^*} . The $v_{i(j^*)}$ and V_{j^*} adopted in the combination and computation of the weights are highlighted in bold, while the other ones are considered with a full or null frequency of occurrence, as well as do not influencing ($P(V_{j^*} = v_{i(j^*)}) = 1$) or cancelling ($P(V_{j^*} = v_{i(j^*)}) = 0$) the combination.

The percentages of the typological parameters present a certain variation, which allows to make some simplifications by excluding some possible combinations. About the parameter V_1 , in all TCs the quasi-totality of the RC units is subdivided between the ones built before the 1980 and the ones built between the 1980 and 2008, while only very few units are successive. This means that, in a faithful application of the proposed procedure, this parameter needs to be accounted in the combination. On the other hand, we decided to exclude the buildings made after the 2008 for several reasons: (i) to reduce the computational efforts hides in the procedure; (ii) being substantial the building stock made before the 2008 in the 5 TCs, an analysis made accounting for only these units (more than the 95% of the units for all TCs) is extremely close to the real situation; (iii) to consider only the older buildings shall provide a conservative result (even if slightly conservative for the case at hand). About the parameter V_3 , it is worth pointing out that the frequency of occurrence of $v_{i(3)}$ are equal to the ones observed for V_9 ($v_{i(9)}$). This situation does not automatically

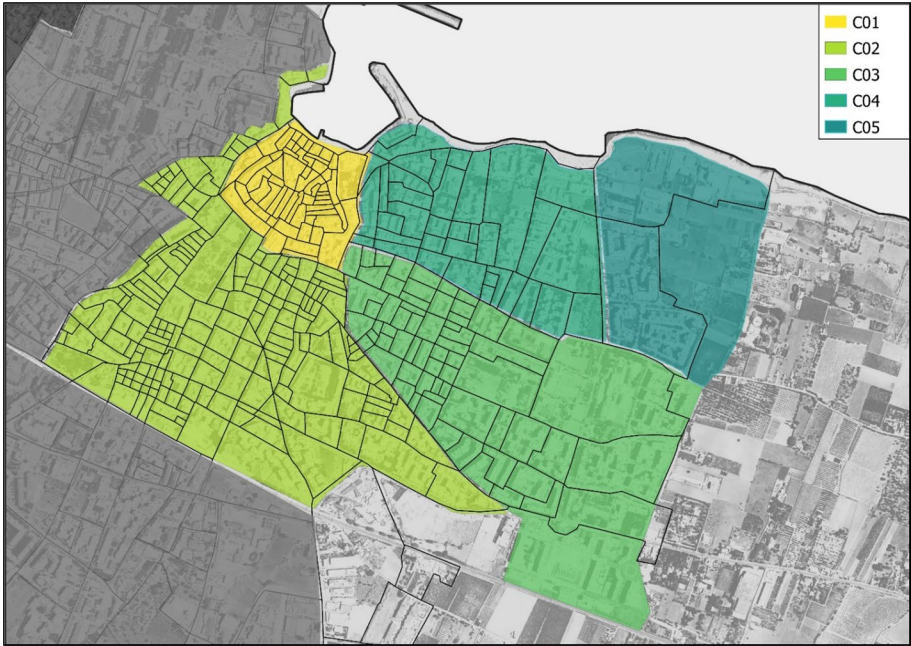


Fig. 5 Areal view of C01, C04 and C04, showing census sections

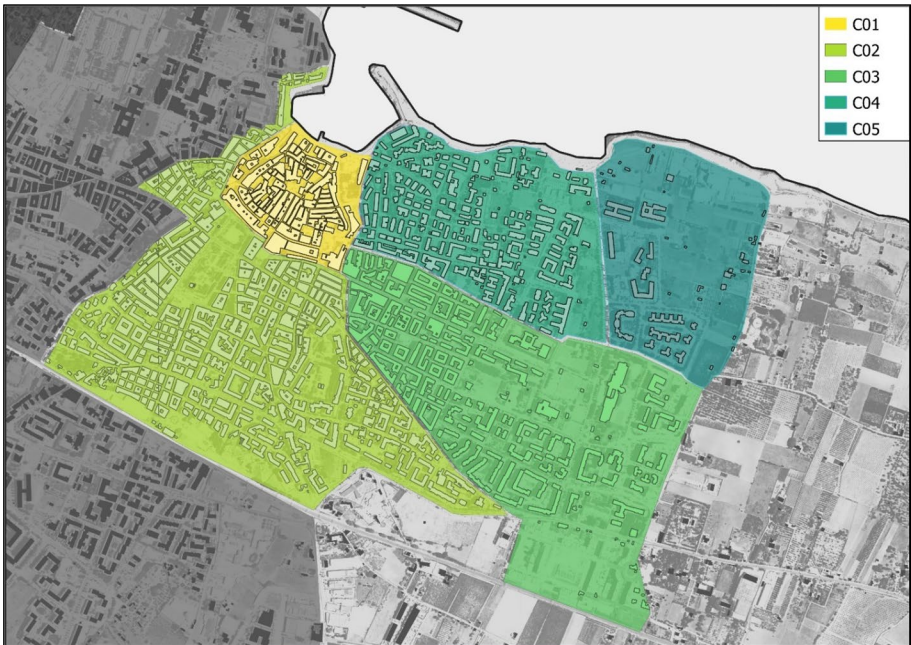


Fig. 6 Areal view of C01, C04 and C04, showing CTR



Fig. 7 Labelled photos of RC buildings taken through VULMA from C04 (left) and C05 (right)

exclude V_3 from the combination but, from the observation of the photos for all 846 buildings for the 5 TCs, it was seen that buildings having a base area higher than 400 m^2 present more than 5 openings per floor while in the case of base area lower than 200 m^2 , the number of openings were lower than 3. Same observation occurs for buildings having base area comprised between 200 and 400 m^2 , which present openings in a range from 3 to 5. This means that there is no chance to combine all $v_{i(j^*)}$ for the parameters V_3 and V_9 but the two parameters are implicitly dependent variables (one parameter between V_3 and V_9 must be excluded). V_4 , V_6 , V_8 and V_{10} present about the 100% of the possibility for one v_i , while V_5 and V_7 present variation. In the end, V_{11} , V_{12} and V_{13} present the 100% of the possibility for one value of $v_{i(j^*)}$ for C01, while they report few sporadic cases of buildings without overhangs and with irregularities. Also in this case, we decided to exclude from the combinations the possibility to have structural irregularities and absence of overhangs, because negligible aspects compared to the observations on the entire building stock. Given the V_{j^*} and $v_{i(j^*)}$ to combine, by applying Eq. 11, T is equal to 72, which is the number of initial realizations to make. For each realization, a variability of the design parameters, e.g., geometrical and mechanical ones, is introduced (see Sect. 4.2). In this way, the number of models for each realization increases for a better consideration of both inter- and intra-building variabilities. Still, by applying Eqs. 12–14, all T values of w_z can be computed for each TC, as reported in Table 3 (each realization is indicated with R_y). The computed value of w_z for each realization will be extended to all models under that typological representation for the estimation of the TC seismic overall fragility.

4.2 Definition of the realizations: modelling and analysis

Once the main typological parameters of realizations were defined, modelling and analysis phases were performed. Concerning to the modelling, a simulate design procedure was developed, aimed to use all typological parameters and to define the missing geometrical and mechanical quantities. As general rules, given the base area of the building, the admissible maximum length of the bays in both main directions (X and Y) is equal to 5 m. For simulating low-, mid- and high-rise buildings, the realizations were conceived as having 3 storeys, 5 storeys and 7 storeys, respectively. The loads were assumed as typical of

Table 2 Total number of RC buildings for C01, C02, C03, C04 and C05 and frequency of occurrence in percentage terms of all v_{ij^*} for each V_{j^*}

Typological parameter (V_{j^*})	Values (v_{ij^*})	Percentages of v_{ij^*} per TCs (%)				
		C01	C02	C03	C04	C05
Number of RC buildings		39	307	275	177	48
Year of construction (V_1)	< 1980 (v_1)	98	89	71	78	79
	1980–2008 (v_2)	2	10	28	20	18
	> 2008 (v_3)	0	1	1	1	3
Number of storeys (V_2)	Low-rise (v_1)	33	30	41	28	54
	Mid-rise (v_2)	64	65	55	62	45
	High-rise (v_3)	3	5	4	10	1
Base area (V_3)	< 200 m² (v_1)	85	75	60	58	65
	> = 200 m²; < 400 m² (v_2)	14	18	28	28	15
	> = 400 m² (v_3)	1	7	12	14	20
Presence of masonry infills (V_4)	Yes (v_1)	100	100	100	100	100
	No (v_2)	0	0	0	0	0
Presence of pilotis floor (V_5)	Yes (v_1)	20	10	25	33	50
	No (v_2)	80	90	75	67	50
Presence of basement floor (V_6)	Yes (v_1)	0	0	0	0	0
	No (v_2)	100	100	100	100	100
Presence of higher ground floor (V_7)	Yes (v_1)	33	35	40	25	7
	No (v_2)	67	65	60	75	93
Presence of superelevation floor (V_8)	Yes (v_1)	0	0	0	0	0
	No (v_2)	100	100	100	100	100
Number of openings per floor (V_9)	< 3 (v_1)	85	75	60	58	65
	> = 3; < 5 (v_2)	14	18	28	28	15
	> = 5 (v_3)	1	7	12	14	20
Type of roof floor (V_{10})	Flat (v_1)	100	100	100	100	100
	Pitched (v_2)	0	0	0	0	0
Presence of overhangs (V_{11})	Yes (v_1)	100	98	100	92	95
	No (v_2)	0	2	0	8	5
Regularity in-plan (V_{12})	Yes (v_1)	100	100	98	100	95
	No (v_2)	0	0	2	0	5
Regularity in-height (V_{13})	Yes (v_1)	100	100	97	100	98
	No (v_2)	0	0	3	0	2

The v_{ij^*} and V_{j^*} adopted in the combination of the weights are reported in bold

residential buildings, where G (gravity load) was assumed equal to 5 kN/m² and Q (live load) was assumed equal to 2 kN/m². The influence of the overhangs was simulated as distributed loads on the external beams. Given the geometry and loads, a simulate design was performed to define the external sections of all structural elements (e.g., beams and columns), by means of the admissible stress method. In this phase the parameter V_1 was considered, where for structures pre-1980 no seismic details and no moment-frames in the slab direction were taken into account, while for structures post-1980, the above aspects were considered. Still, according to the older Italian seismic codes (pre- and post-1980), the

Table 3 Outputs given by the combination of V_j and $v_{j(i^*)}$ and the computation of w_z and accounting for the variation of V_1, V_2, V_3, V_5 and V_7 (72 values for each TC, subdivided in 2 columns)

R_y	w_z per TC—Eqs. 12–14									
	C01	C02	C03	C04	C05					
R_1	0.00037	0.00075	0.00087	0.00161	0.00713	0.01070	0.00281	0.00844	0.00258	0.03428
R_2	0.01814	0.03684	0.00701	0.01302	0.01747	0.02620	0.01045	0.03135	0.00971	0.12894
R_3	0.00072	0.00146	0.00188	0.00349	0.00957	0.01436	0.00623	0.01869	0.00215	0.02856
R_4	0.03519	0.07144	0.01519	0.02820	0.02343	0.03515	0.02314	0.06942	0.00809	0.10745
R_5	0.00003	0.00007	0.00014	0.00027	0.00070	0.00104	0.00100	0.00301	0.00005	0.00063
R_6	0.00165	0.00335	0.00117	0.00217	0.00170	0.00256	0.00373	0.01120	0.00018	0.00239
R_7	0.00006	0.00012	0.00021	0.00039	0.00333	0.00499	0.00136	0.00407	0.00060	0.00791
R_8	0.00299	0.00607	0.00168	0.00312	0.00815	0.01223	0.00505	0.01514	0.00224	0.02976
R_9	0.00012	0.00024	0.00045	0.00084	0.00447	0.00670	0.00301	0.00902	0.00050	0.00659
R_{10}	0.00580	0.01177	0.00364	0.00677	0.01093	0.01640	0.01117	0.03351	0.00187	0.02480
R_{11}	0.00001	0.00001	0.00003	0.00006	0.00032	0.00049	0.00049	0.00146	0.00001	0.00015
R_{12}	0.00027	0.00055	0.00028	0.00052	0.00080	0.00119	0.00180	0.00541	0.00004	0.00055
R_{13}	0.00044	0.00088	0.00008	0.00015	0.00143	0.00214	0.00068	0.00204	0.00079	0.01055
R_{14}	0.02134	0.04334	0.00065	0.00121	0.00349	0.00524	0.00252	0.00757	0.00299	0.03967
R_{15}	0.00084	0.00172	0.00018	0.00033	0.00191	0.00287	0.00150	0.00451	0.00066	0.00879
R_{16}	0.04140	0.08405	0.00142	0.00263	0.00469	0.00703	0.00559	0.01676	0.00249	0.03306
R_{17}	0.00004	0.00008	0.00001	0.00003	0.00014	0.00021	0.00024	0.00073	0.00001	0.00020
R_{18}	0.00194	0.00394	0.00011	0.00020	0.00034	0.00051	0.00090	0.00270	0.00006	0.00073
R_{19}	0.00148	0.00301	0.00780	0.01448	0.02140	0.03210	0.00571	0.01714	0.00258	0.03428
R_{20}	0.07257	0.14734	0.06308	0.11715	0.05240	0.07860	0.02122	0.06365	0.00971	0.12894
R_{21}	0.00287	0.00583	0.01689	0.03137	0.02871	0.04307	0.01265	0.03795	0.00215	0.02856
R_{22}	0.14074	0.28575	0.13667	0.25382	0.07029	0.10544	0.04698	0.14095	0.00809	0.10745
R_{23}	0.00013	0.00027	0.00130	0.00241	0.00209	0.00313	0.00204	0.00612	0.00005	0.00063

Table 3 (continued)

R_y	w_z per TC—Eqs. 12–14									
	C01	C02	C03	C04	C05	C06	C07	C08	C09	C10
R_{24}	0.00660	0.01340	0.01952	0.00767	0.00758	0.02273	0.00018	0.00239		
R_{25}	0.00024	0.00050	0.00347	0.01498	0.00276	0.00827	0.00060	0.00791		
R_{26}	0.01195	0.02427	0.02812	0.03668	0.01024	0.03073	0.00224	0.02976		
R_{27}	0.00047	0.00096	0.00753	0.02010	0.00611	0.01832	0.00050	0.00659		
R_{28}	0.02318	0.04707	0.06092	0.04920	0.02268	0.06804	0.00187	0.02480		
R_{29}	0.00002	0.00005	0.00058	0.00146	0.00098	0.00295	0.00001	0.00015		
R_{30}	0.00109	0.00221	0.00469	0.00358	0.00366	0.01098	0.00004	0.00055		
R_{31}	0.00174	0.00354	0.00135	0.00642	0.00138	0.00414	0.00079	0.01055		
R_{32}	0.08538	0.17334	0.01093	0.01572	0.00512	0.01536	0.00299	0.03967		
R_{33}	0.00338	0.00686	0.00293	0.00861	0.00305	0.00916	0.00066	0.00879		
R_{34}	0.16558	0.33618	0.02369	0.02109	0.01134	0.03402	0.00249	0.03306		
R_{35}	0.00016	0.00032	0.00023	0.00063	0.00049	0.00148	0.00001	0.00020		
R_{36}	0.00776	0.01576	0.00182	0.00153	0.00183	0.00549	0.00006	0.00073		

compressive and tensile admissible stresses of concrete and steel reinforcement were supposed according to the code prescriptions. To design columns, the simple axial stress (N) was considered. The section of a generic column (A_c) was obtained by the ratio between the load acting on that column and the admissible stress of concrete, σ_c . The value of N varied on the base of the columns' position (internal columns are doubly loaded than external ones). To design beams, both deep (external frames) and wide shallow (internal frames) beams were considered, in which section sides and simple steel reinforcement were determined through the definition of the maximum bending moment stress (M_{max}), quantified according to a scheme of fixed ends beam, for simplicity. Shear reinforcement of beams and columns was computed according to the minimum requirements of the adopted building codes.

In addition, external masonry infills were considered as interacting with the enclosing frames and the infill thickness was imposed in a range from 30 to 40 cm, according to the size of the external columns. When columns' sides exceeded those values (especially in tall buildings), masonry infills of 40 cm thick was assumed. Finally, the design and the influence of foundations were neglected and no RC walls and stairs were employed.

To account for variabilities, each of the 72 models was simulated by parametrically varying the features reported in Table 4, according to the old Italian design practice and following the strategy employed in Leggieri et al. (2021). In particular, for pre-1980 buildings ($V_I = v_{I(1)}$), two extreme values for σ_c were selected and they were equal to 4 and 5 Mpa, while for post-1980 buildings ($V_I = v_{2(I)}$), the adopted extreme values were assumed equal to 6 and 7.5 Mpa. For both pre- and post-1980 structures, two values for the plan aspect-ratio, AR (1:1 and 1:2, having square and rectangular in-plan shapes, respectively) and two values for strong masonry infill properties (compression strength, σ_m equal to 2.5 MPa and 1.5 Mpa, according to the most recurrent features in the observed area and according to Uva et al. 2012 and Hak et al. 2012, respectively) were considered. Still, for each range of V_3 , two values of base area were employed (100 and 200 m² for $V_3 = v_{I(3)}$; 300 and 400 m² for $V_3 = v_{2(3)}$; 500 and 600 m² for $V_3 = v_{3(3)}$). Finally, some parameters were varied, considering the expected low influence in the final results, e.g., the admissible stress of steel reinforcement, σ_s , (as shown in Stefanini et al. 2022), which was assumed equal to 140 MPa (smooth bars) and 220 MPa (corrugated bars), for pre- and post-1980 structures, respectively.

Considering the varied parameters in the simulation of realizations and their combination, 16 numerical models were generated for each of the 72 models, for a total of 1152 models. It is worth mentioning that this approach could be even more refined by considering geometrical and mechanical parameters as random variables, especially if real data are available for the accounted features (which is not the case herein presented). In this case, the computational effort could strongly increase, especially for running nonlinear dynamic

Table 4 Geometrical and mechanical parameter varied for each realization. Vector indicates the values adopted in the simulation.

Parameter	Pre-1980 buildings	Post-1980 buildings
σ_c (MPa)	[4 5]	[6 7.5]
σ_m (MPa)	[1.5 2.5]	
AR	[1:1 1:2]	
Area (m ²)	[100 200 300 400 500 600]	

For the parameter area, all values are considered and they were sampled according to the ranges in Table 2

analyses to intensively explore the seismic performance of a building portfolio typologically defined. Anyway, it is possible reduce the computational weight by employing adequate simulation technique strategies (e.g., Vorechovský and Novák 2009).

After, all realizations were implemented in OpenSees (McKenna 2011) where beams and columns were modelled as one-dimensional frame elements, fixed restraints were positioned at the base of the columns and a rigid diaphragm was imposed at each floor. To account for the nonlinear behaviour, a lumped plasticity approach was adopted, by placing plastic hinges to the end sections of the structural elements (*beamWithHinges* elements). Plastic hinges were characterized by an in-cycle degrading backbone and moderately pinching hysteresis without cyclic degradation. Inelastic mechanisms were assumed as ductile, by considering the combination of axial and bending stresses for columns and only bending for beams. For columns, the axial stresses were obtained by employing a seismic combination of vertical loads, given by the prescriptions proposed by Eurocode 8. In numerical models, columns hinges took into account a bi-directional behaviour while mono-directional hinges were assigned to the beams. Each plastic hinge was defined according to the Eurocode 8 approach, by evaluating for each section a quadrilinear moment-rotation constitutive law and by characterizing the hysteretic behaviour with four linear branches: first cracking of concrete, yielding of longitudinal bars with hardening, softening for simulating the strength degradation and a residual plateau, fixed at 20% of the yielding moment. For each plastic hinge, chord rotation values provided the achievement of limit-states, as well as the 75% of the ultimate rotation for the life safety (LS) limit-state and the ultimate rotation for the near collapse (NC) limit-state. No shear hinges were accounted for avoiding convergence problems but, at the same time, the shear mechanisms control was performed a posteriori. The influence of infill panels was considered by adopting a strut modelling with two cross braces in each frame (*corotationalTruss* elements, as in Ruggieri et al. 2019), able to simulate the compressive stress on a diagonal path under vertical and horizontal actions. The nonlinear behaviour of the struts was defined by using the formulations proposed in Panagiotakos and Fardis (1996) and only in plane-mechanisms were considered. Finally, local effects on beam-columns joints were neglected.

For purpose of validation, the above simulate design procedure and the subsequent modelling approach were compared with the work by Verderame et al. (2010), in which authors proposed an automated procedure to investigate the seismic capacity of existing RC buildings in Southern Italy. In particular, the paper presented the simulation of some buildings for a specific class, providing the dimensions of structural elements and the results of pushover analyses. Figure 8 shows the plan of one of the simulated buildings in Verderame et al. (2010), constituted by a rectangular in-plan shape with sides of 27 m × 15 m, 7 bays in X direction, 3 bays in Y direction, 4 storeys with higher ground floor, σ_c equal to 7.5 MPa, and σ_s equal to 180 MPa. In this case, no masonry infill panels were considered. Using these data, the simulation was performed according to the method proposed in this paper and the section of the beams and columns are reported in Fig. 8.

Observing the obtained results some few differences occur, in terms of structural elements section sides, steel reinforcement and bays length. On the other hand, by performing pushover analyses in both main directions (Fig. 9), it is possible to denote a good matching between the two simulated buildings behaviour, also considering the different modelling strategy employed in Verderame et al. (2010) and the different constitutive law adopted for plastic hinges of structural elements.

In Figs. 10 and 11, the schemes of some numerical models under a specific realization are reported (4 configurations, adopting two values of AR and two values of base area). Figure 10 shows R_1 , characterized by 3 storeys, base area lower than /equal to

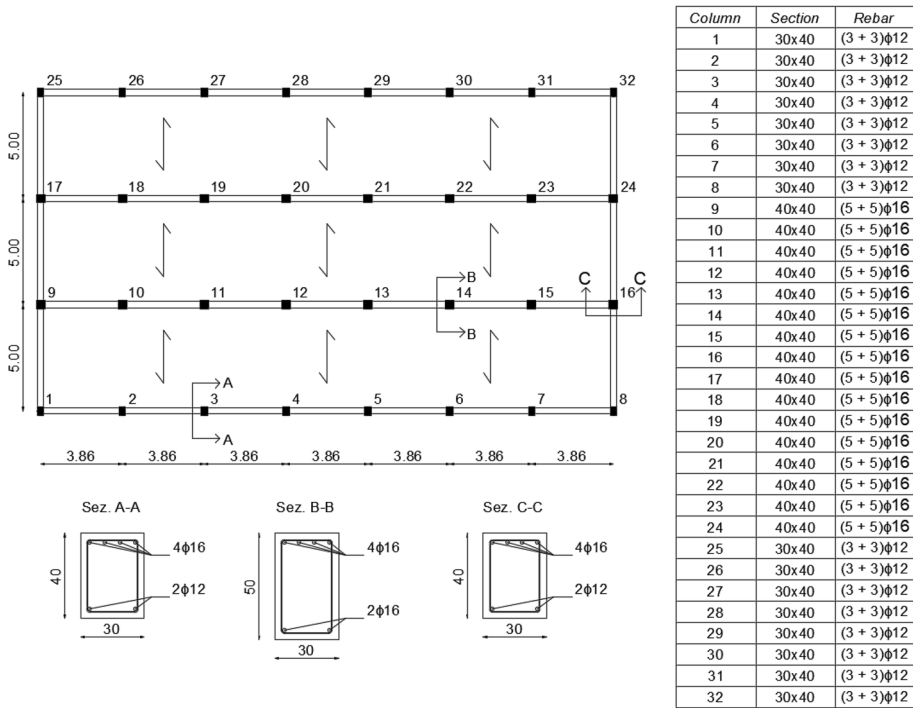


Fig. 8 Validation of the proposed simulation approach according to geometrical and mechanical parameters of a building typology reported in Verderame et al. (2010), in which some differences can be observed in terms of structural elements’ dimensions, steel reinforcement and bays length

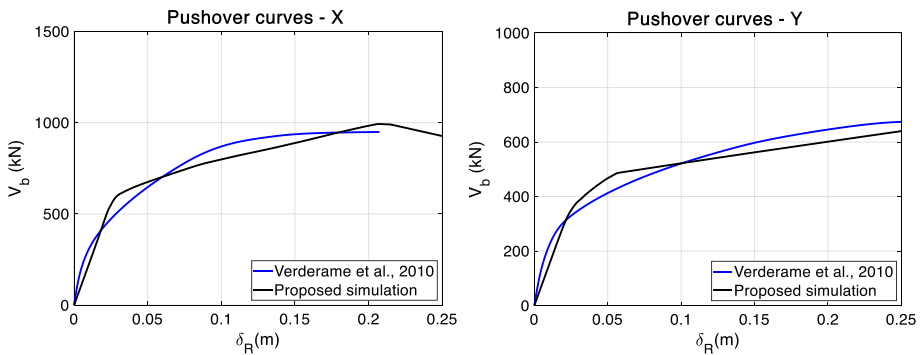


Fig. 9 Validation of the proposed simulation approach and comparison of pushover with results proposed by Verderame et al. (2010). Although different modelling assumptions, similar linear and nonlinear behaviour can be observed

200 m², year of construction before the 1980, without pilotis and higher ground floor. Figure 11 shows R_{72} , characterized by 7 storeys, base area greater than 400 m², year of construction after the 1980, with pilotis and higher ground floor.

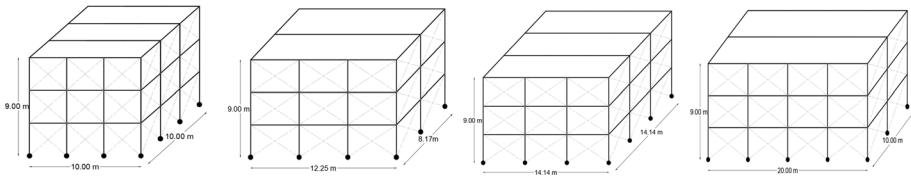


Fig. 10 Scheme of numerical models for R_1 , characterized by 3 storeys, base area lower than/equal to 200 m^2 , year of construction before the 1980, without pilotis and higher ground floor (masonry infills are considered on the external sides of buildings). For each geometrical configuration, 2 values of AR , 2 values of σ_c and 2 values of σ_m were employed, for a total of 16 models

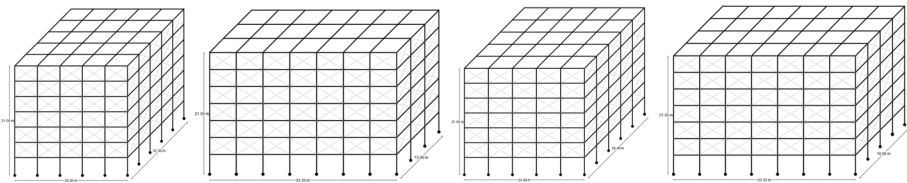


Fig. 11 Scheme of numerical models for R_{72} , characterized by 7 storeys, base area higher than 400 m^2 , year of construction after the 1980, with pilotis and higher ground floor (masonry infills are considered on the external sides of buildings excluded the first floor). For each geometrical configuration, 2 values of AR , 2 values of σ_c and 2 values of σ_m were employed, for a total of 16 models

After modelling, eigenvalue analyses were run, in order to estimate the main periods of realizations. Looking at the entire sample of models, the main periods range from 0.22 to 1.14 s, result that in a view of overall fragility drives to the selection of a unique IM for all realizations. Hence, as just mentioned in Sect. 3.5, $AvgSa$ was assumed as IM, considering a range of spectral accelerations from a period of 0.1 s to a period of 3.0 s, with a step of 0.1 s. To investigate the seismic performance of all realizations, cloud analyses were performed on numerical models, by using the set of 30 natural ground motion records with two horizontal components, taken from the medium seismicity set provided by the INNO-SEIS project (Kohrangi and Vamvatsikos 2016). Assuming as EDP the θ_{max} , the maximum value recorded between the two main directions (X and Y) was selected, in order to represent in a unique plane (IM-EDP) the seismic response of all realizations. To define a general building-level limit-state, several criteria can be adopted, accounting for the brittle and ductile collapse of single or more structural elements, as defined in Ruggieri et al. (2021b). For the case at hand, ductile and brittle mechanisms were accounted for defining the safety level of the realizations, by opting for a single component criterion, echoing the prescriptions of the current Italian building code (NTC 2018). In particular, the ductile collapse of the realization occurs when the first hinge in a column achieves the ultimate rotation while the shear collapse occurs when the first column is subjected to its limit shear capacity. The shear checking was performed in post-processing (check of the maximum shear occurred during analyses on each column and comparison with the values provided by the Italian Building code formulation), being numerical models made as ductile. An oriented criterion to the first component failure could be considered conservative in an assessment phase but, on the other hand, the disposition of ideal buildings (instead of real-life of index ones) brings to avoid any composite rule to define the safety level of simulated structural elements.

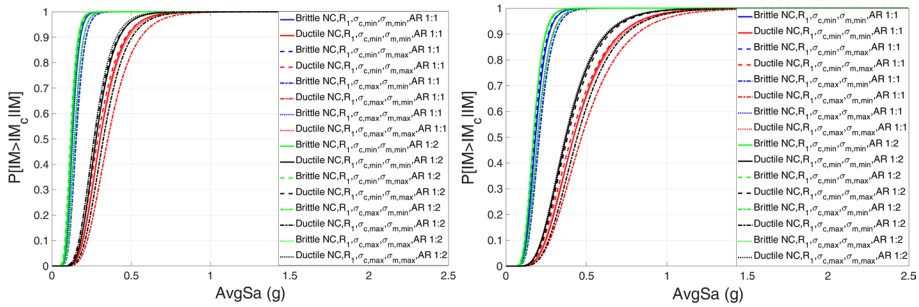


Fig. 12 Fragility curves for brittle and ductile limit-states of R_1 , characterized by 3 storeys, base area lower/equal than 200 m^2 (to left models with area of 100 m^2 , to right models with area of 200 m^2), year of construction before the 1980, without pilotis and higher ground floor, and accounting for all values of AR , σ_c and σ_m

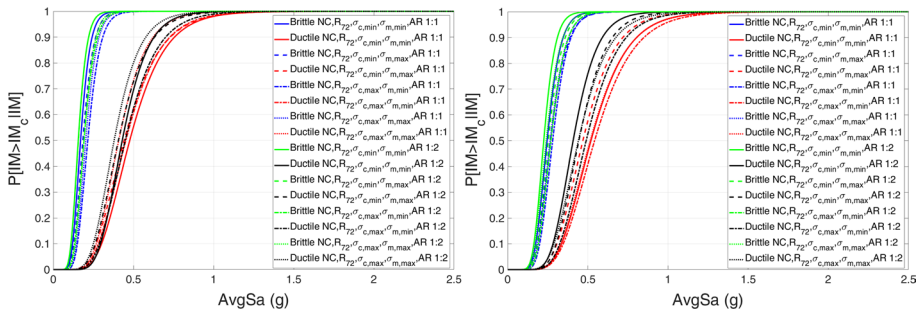


Fig. 13 Fragility curves for brittle and ductile limit-states of R_{72} , characterized by 7 storeys, base area higher than 400 m^2 (to left models with area of 500 m^2 , to right models with area of 600 m^2), year of construction after the 1980, with pilotis and higher ground floor, and accounting for all values of AR , σ_c and σ_m

4.3 Evaluation of realizations fragility curves and influence of seismic input selection

The next step of the procedure is the evaluation of the single fragility curves for each realization. To this scope, after running cloud analyses the trend of the structural behaviour on the IM-EDP plane was estimated by using the power law approximation provided by Cornell et al. (2002). The fragility curves for each realization were computed accounting for the safety limit-states (brittle and ductile NC), selecting as EDP threshold the minimum value between the ones occurred in the main horizontal directions (X and Y). Still, to account for the dispersion of each fragility curve, an additional epistemic uncertainty was always considered, due to the several factors, such as the adopted modelling approach, the design simulation and the quality of available data. Despite several recommendations are proposed in the scientific literature (e.g., O’Reilly and Sullivan 2018), a fixed value of 20% was imposed for all realizations and both safety limit-states.

In Figs. 12 and 13, fragility curves for brittle and ductile limit-states are shown, with regard to R_1 and R_{72} . In both Figures, two graphs are reported showing all fragility curves grouped for base area. Blue and red curves indicate fragility curves for AR of 1:1 for brittle and ductile limit-states, respectively; green and black curves indicate fragility curves for

AR of 1:2 for brittle and ductile limit-states, respectively. Table 5 reports the values of μ_y and β_y for each fragility curve of R_1 and R_{72} and the indication of the parameters varied in the modelling (full data are provided in the Supplementary Material file). Looking at the results of the single fragility curves some observations can be highlighted, given by the comparisons among the values of μ_y and β_y . In particular, looking at the year of construction, the realizations designed according to code prescriptions post-1980 present higher

Table 5 Results of fragility curves (μ_y and β_y) for R_1 and R_{72} , accounting for brittle and ductile limit-states, obtained by varying the year of construction (Yc), the number of storeys (Nst), the higher ground floor (Hgf), the pilotis floor (Plt), the base area (A), the aspect ratio (AR), the admissible stress of concrete (σ_c) and the admissible stress of masonry (σ_m)

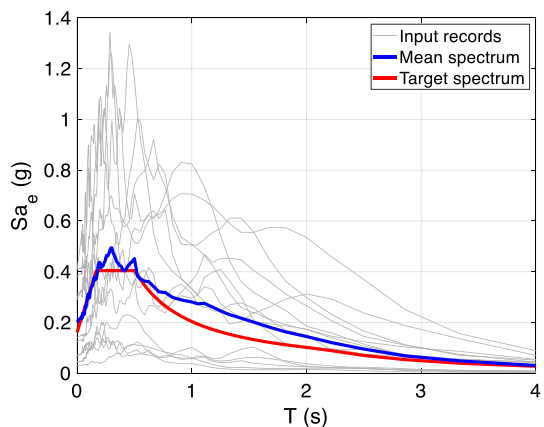
R_y	Yc	Nst	Hgf	Plt	$A(m^2)$	AR	σ_c (Min–Max)	σ_m (Min–Max)	Brittle		Ductile	
									μ_y	β_y	μ_y	β_y
R_1	<1980	3	No	No	100	1:1	Min	Min	0.129	0.26	0.304	0.35
	<1980	3	No	No	100	1:1	Min	Max	0.121	0.28	0.289	0.37
	<1980	3	No	No	100	1:1	Max	Min	0.153	0.27	0.353	0.36
	<1980	3	No	No	100	1:1	Max	Max	0.142	0.27	0.304	0.36
	<1980	3	No	No	100	1:2	Min	Min	0.121	0.25	0.278	0.33
	<1980	3	No	No	100	1:2	Min	Max	0.116	0.28	0.267	0.35
	<1980	3	No	No	100	1:2	Max	Min	0.146	0.26	0.324	0.34
	<1980	3	No	No	100	1:2	Max	Max	0.127	0.26	0.264	0.34
	<1980	3	No	No	200	1:1	Min	Min	0.183	0.30	0.420	0.41
	<1980	3	No	No	200	1:1	Min	Max	0.175	0.32	0.406	0.44
	<1980	3	No	No	200	1:1	Max	Min	0.207	0.31	0.470	0.43
	<1980	3	No	No	200	1:1	Max	Max	0.196	0.31	0.420	0.43
	<1980	3	No	No	200	1:2	Min	Min	0.171	0.28	0.373	0.41
	<1980	3	No	No	200	1:2	Min	Max	0.169	0.30	0.383	0.41
	<1980	3	No	No	200	1:2	Max	Min	0.199	0.31	0.443	0.40
	<1980	3	No	No	200	1:2	Max	Max	0.171	0.29	0.368	0.41
R_{72}	>1980	7	Yes	Yes	500	1:1	Min	Min	0.170	0.27	0.477	0.36
	>1980	7	Yes	Yes	500	1:1	Min	Max	0.184	0.28	0.442	0.39
	>1980	7	Yes	Yes	500	1:1	Max	Min	0.215	0.28	0.452	0.37
	>1980	7	Yes	Yes	500	1:1	Max	Max	0.202	0.27	0.408	0.33
	>1980	7	Yes	Yes	500	1:2	Min	Min	0.156	0.27	0.430	0.30
	>1980	7	Yes	Yes	500	1:2	Min	Max	0.156	0.27	0.406	0.34
	>1980	7	Yes	Yes	500	1:2	Max	Min	0.192	0.29	0.449	0.35
	>1980	7	Yes	Yes	500	1:2	Max	Max	0.191	0.26	0.380	0.33
	>1980	7	Yes	Yes	600	1:1	Min	Min	0.246	0.27	0.520	0.34
	>1980	7	Yes	Yes	600	1:1	Min	Max	0.267	0.29	0.469	0.33
	>1980	7	Yes	Yes	600	1:1	Max	Min	0.281	0.27	0.542	0.35
	>1980	7	Yes	Yes	600	1:1	Max	Max	0.265	0.28	0.515	0.35
	>1980	7	Yes	Yes	600	1:2	Min	Min	0.225	0.25	0.408	0.29
	>1980	7	Yes	Yes	600	1:2	Min	Max	0.254	0.27	0.444	0.30
	>1980	7	Yes	Yes	600	1:2	Max	Min	0.270	0.27	0.490	0.32
	>1980	7	Yes	Yes	600	1:2	Max	Max	0.240	0.28	0.441	0.33

σ_c and σ_m are expressed in terms of Min/Max, referring to the values in Table 4

medians and lower dispersions than the ones designed according to code prescriptions pre-1980, both for ductile and brittle mechanisms. Buildings with more compact shapes are less vulnerable (e.g., lower storeys and AR of 1:1). Indeed, as expected, buildings with pilotis and higher ground floor presents lower medians than the cases in which both of them are absent, both for brittle and ductile mechanisms. When only higher ground floor is present, the medians are similar to the case without it. Assuming same mechanical parameters and number of storeys, buildings with lower base area are less vulnerable. In the end, buildings with higher values of σ_c presents higher values of the individual medians, while stronger infills (σ_m) increases the vulnerability.

Another aspect to highlight in the overall evaluation of single fragility curves regards the selection of the seismic input. As a matter of fact, considering the observed scale of analysis, the seismic input can be accurately characterized accounting for available microzonation and soil amplification. For the above analyses, a set of medium intensity records was considered, while it is possible to improve the evaluation by performing a record selection according to the definition of the target spectrum of the municipality and the related amplifications factors. Accounting for recent studies about the topic and looking at the national microzonation, Falcone et al. (2021) and Mendicelli et al. (2022) provided maps of amplification factors for three intervals of periods, PGA and peak ground velocity (PGV), basing on the IGAG_20 procedure and allowing to consider the ground motion modification induced by the stratigraphic effect. For the purpose of this paper, authors considered the data provided by Mori et al. (2020), which released a new $V_{s,30}$ (shear wave velocity) Italian map. Therefore, a ground motion record selection can be performed and analyses on typological realizations can be carried out according to the proposed framework, considering a specific target spectrum and related soil amplification. For the sake of synthesis, the new analyses were performed only on some of the models related to R_I and R_{72} , in order to gain some new insights from the extremes of the performed numerical campaign. For the case at hand, according to the microzonation map, the municipality of Bisceglie presents a value of $V_{s,30}$ ranging from 640 to 760 m/s. Hence, according to the Eurocode classification, the soil category to consider is of type B. A record selection was performed through the tool Rexel (Iervolino et al. 2010), employing the Eurocode 8 provisions. In particular, differences between mean and target spectra amounted to +30% and -10%, while the fitting was performed between 0.2 and 1.2 s, according to the period ranges in which realizations interpose. Figure 14 shows graphs reporting a set of 14 elastic ground motions

Fig. 14 Elastic acceleration spectra of the selected set of records, mean spectrum and target spectrum, all for 5% damping



spectra (grey lines), the obtained mean spectrum (blue line) and the considered target spectrum (red line), all for 5% damping (S_{a_c} indicates the elastic acceleration).

Using the selected set of ground motion records, new analyses were performed on some numerical models related to R_1 and R_{72} . Of interest is to compare fragility curves with the different seismic inputs, also considering the different number of ground motion records adopted. The results are summarized in Fig. 15, where blue and red curves indicate models analysed with the previous seismic input, while light blue and magenta curves indicate models analysed with the new seismic input. Details on geometrical and mechanical properties of the models are provided in the caption of Fig. 15.

Results show that assuming seismic input according to amplified target spectrum, more vulnerable fragility curves were obtained, both for brittle and ductile limit-states. The differences were more amplified for brittle limit states, while for ductile limit states higher dispersions were obtained. Although the different seismic input, the trend of the models remains unchanged, considering more vulnerable models designed according to code prescriptions pre-1980, lower values of σ_c and higher values of σ_m . In the end, observing the obtained results, the seismic input assumes a key role in fragility analysis as also reported in the scientific literature. However, for the aim of the proposed procedure to evaluate seismic overall fragility for TCs, the small differences observed among individual fragility curves and the large number of numerical results to combine suggest that also the adopted approach for seismic input selection can provide acceptable results.

4.4 Evaluation of overall seismic fragility curves for town compartments

Having the parameters of fragility curves and the w_c previously evaluated for each TC of interest (see Table 3), seismic overall fragility curves were evaluated by using the formulations proposed in Eqs. 15–17. The results of weighted procedure are shown in Table 6, where $\mu_{overall}$ and $\beta_{overall}$ are reported for each TC and limit-state, while Fig. 16 shows the graphical outline of the fragility curves.

Looking at the obtained results, overall fragilities return some differences in terms of medians and dispersions. In detail, comparing C01 and C05 the medians increase, with a percentage increment of the 26% for brittle limit-state and 25% for ductile limit-state.

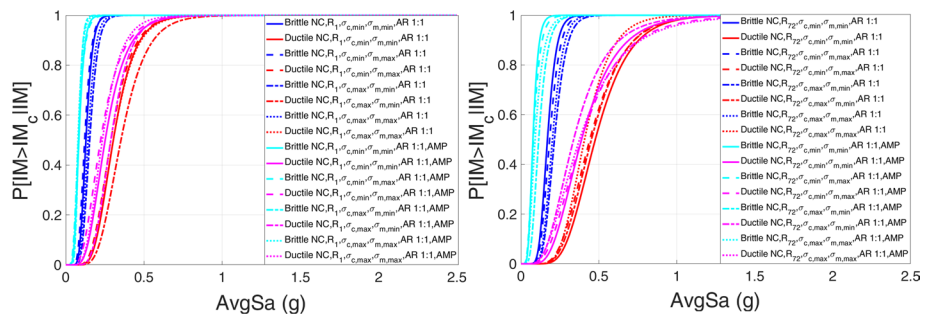


Fig. 15 To the left, fragility curves for brittle and ductile limit-states of R_1 , characterized by 3 storeys, base area equal to 100 m², year of construction before the 1980, without pilotis and higher ground floor, and accounting for all values of σ_c and σ_m and for soil amplification (AMP). To the right, fragility curves for brittle and ductile limit-states of R_{72} , characterized by 7 storeys, base area equal to 500 m², year of construction after the 1980, with pilotis and higher ground floor, and accounting for all values of σ_c and σ_m and for soil amplification (AMP)

Table 6 $\mu_{overall}$ and $\beta_{overall}$ of the overall fragility curves for all investigated TCs and limit-states

Weighted overall fragility curves	Brittle NC limit-state		Ductile NC limit-state	
	$\mu_{overall}$	$\beta_{overall}$	$\mu_{overall}$	$\beta_{overall}$
C01	0.132	0.30	0.294	0.35
C02	0.139	0.31	0.312	0.37
C03	0.159	0.32	0.353	0.39
C04	0.164	0.32	0.364	0.39
C05	0.178	0.33	0.392	0.41

Same trend is observed for the dispersions that increase at a slower rate than medians. The obtained result confirms the powerful of the proposed procedure considering that, although a certain homogeneity of the different building portfolios, C05 is the newest TC and presents lower vulnerability while C01 is the oldest TC and presents higher vulnerability. The obtained results depend on the weight and the values that each realization assumes in the computation of the overall fragility curves, also according to the parameters employed in the numerical models. The results of C01 are strongly conditioned by the mid-rise realizations designed through pre-1980 building code. In C02, C03 and C04 this effect is attenuated, with an increasing number of low- and mid-rise buildings designed after the 1980 and higher base area. C05 presents lower vulnerability than the previous TCs, given by a large part of the buildings designed after the 1980 and having low number of storeys and a lower base area. Nevertheless, the obtained difference between the first and the last TCs is not extremely high, given by the evidence that the greater part of the newer buildings is designed with pilotis and higher ground floor. Also looking at the dispersions, the results are similar for all TCs and relatively low, considering the elevated number of analyses (intra-building variability) and realizations (inter-building variability) accounted in the presented analysis.

5 Conclusions and further developments

An analytical-mechanical based framework to estimate seismic overall fragility curves for homogeneous TCs is presented. The approach is proposed by means of an analytical procedure that allows to account for all typological parameters constituting the focused building portfolios, on the base of ideal mechanical models. In detail, the steps of the procedure are: (1) data collection of data by exploiting multisource data (e.g., CARTIS, VULMA); (2) identification of the main typological parameters and statistical analysis of the collected data, by defining the percentage of occurrence of each parameter and the related observed values; (3) combination of the typological parameters to create ideal buildings, herein named realizations, and definition of the weight that each realization assumes in the TC using the law of compound probability; (4) modelling and analysis of the realizations, accounting for nonlinear properties and using dynamic analyses; (5) definition of single fragility curves for each ideal model; (6) definition of the seismic overall fragility curve, by applying a weighted approach of the laws of total variance and total expectation. The proposed approach was applied on the case study of Bisceglie municipality, Puglia, Southern Italy, by referring to the RC building portfolios of 5 TCs.

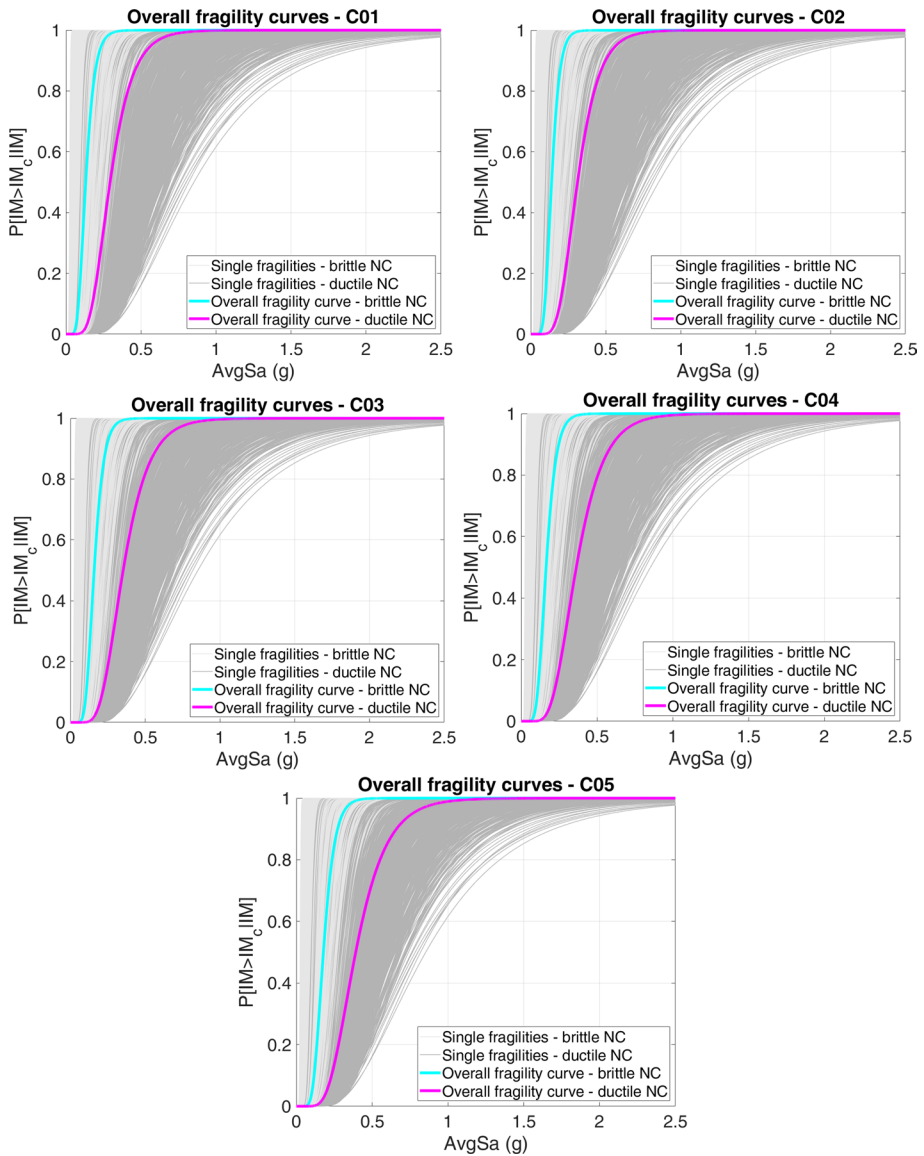


Fig. 16 Overall fragility curves for C01, C02, C03, C04 and C05 and accounting for the brittle and ductile NC limit-states

The obtained results in terms of overall fragility curves show that going from the older TC (C01) to newer one (C05), the medians and the dispersions increase, evidence that confirms the effectiveness of the proposed procedure in the estimation of the seismic behaviour of building portfolios on typological base. In particular, the results for older TCs are conditioned by the mid-rise numerical models designed according to pre-1980 building code, while for the main recent TCs, the evaluations are ruled by the more compact buildings (lower number of storeys and a lower base area) designed according

post-1980 building code. In the end, the differences between the first and last TCs is not extremely high, given by the presence of pilotis and higher ground floor in newer buildings. Observing the achievements of the paper, the main advantages of the proposed procedure can be summarized as follows:

- The procedure allows of avoiding an a-priori selection of one or more index buildings to represent the specific building portfolio, as well as to assume an established building taxonomy.
- The procedure is based on the collection of multi-source data, which can be aggregated in order to generate significant mechanical models. Those data, if individually considered, could be not enough for a detailed modelling process.
- The procedure is simply expandible to other classes and typologies of buildings, despite herein is applied on RC buildings, and the numerical realizations can be used for simulating the overall fragilities of building portfolios in other areas presenting same typological parameters.
- The procedure accounts for intra-buildings and inter-buildings parameters of the building portfolios, by exploiting a new weighted formulation.
- The obtained results on the case study show a certain reliability of the method, also with regard to the safety limit-states, which returns conclusions in accordance with the observed typological parameters in the area and that influence the seismic behaviour of the building portfolios under investigations.

Finally, several aspects should be improved in future developments, such as the reduction of the computational efforts required to model all possible realizations given by the performed combinations and the number of analyses to run for reducing uncertainty sources. Influence of ground motion selection and soil amplification can be accounted for improving the evaluation of the seismic overall fragility curve, especially when microzonation is available.

Supplementary Information The online version contains supplementary material available at <https://doi.org/10.1007/s10518-022-01516-7>.

Acknowledgements Authors acknowledges funding provided by the Italian Department of Civil Protection in the framework of the national project DPC-ReLUIS 2019-2021.

Funding Open access funding provided by Politecnico di Bari within the CRUI-CARE Agreement. The authors have not disclosed any funding.

Declarations

Competing interests The authors have not disclosed any competing interests.

Open Access This article is licensed under a Creative Commons Attribution 4.0 International License, which permits use, sharing, adaptation, distribution and reproduction in any medium or format, as long as you give appropriate credit to the original author(s) and the source, provide a link to the Creative Commons licence, and indicate if changes were made. The images or other third party material in this article are included in the article's Creative Commons licence, unless indicated otherwise in a credit line to the material. If material is not included in the article's Creative Commons licence and your intended use is not permitted by statutory regulation or exceeds the permitted use, you will need to obtain permission directly from the copyright holder. To view a copy of this licence, visit <http://creativecommons.org/licenses/by/4.0/>.

References

- Aiello MA, Ciampoli PL, Fiore A, Perrone D, Uva G (2017) Influence of infilled frames on seismic vulnerability assessment of recurrent building typologies. *Ingegneria Sismica* 34(4):58–80
- Bakalis K, Vamvatsikos D (2018) Seismic fragility functions via nonlinear response history analysis. *J Struct Eng* 144(10):04018181. [https://doi.org/10.1061/\(ASCE\)ST.1943-541X.0002141](https://doi.org/10.1061/(ASCE)ST.1943-541X.0002141)
- Baker JW (2015) Efficient analytical fragility function fitting using dynamic structural analysis. *Earthq Spectra* 31(1):579–599. <https://doi.org/10.1193/021113EQS025M>
- Borzi B, Faravelli M, Di Meo A (2021) Application of the SP-BELA methodology to RC residential buildings in Italy to produce seismic risk maps for the national risk assessment. *Bull Earthq Eng* 19:3185–3208. <https://doi.org/10.1007/s10518-020-00953-6>
- Borzi B, Pinho R, Crowley H (2008) Simplified pushover-based vulnerability analysis for urban scale assessment of RC buildings. *Eng Struct* 30(3):804–820. <https://doi.org/10.1016/J.ENGSTRUCT.2007.05.021>
- Braga F, Dolce M, Liberatore D. (1982) A statistical study on damaged buildings and an ensuing review of the MSK-76 scale. In: Proceedings of the seventh European conference on earthquake engineering, Athens, Greece, pp. 431–450.
- Brando G, Cianchino G, Rapone D, Spacone E, Biondi S (2021) A CARTIS-based method for the rapid seismic vulnerability assessment of minor Italian historical centres. *Int J Disaster Risk Reduct.* <https://doi.org/10.1016/j.ijdr.2021.102478>
- Brzev S, Scawthorn C, Charleson AW, Allen L, Greene M, Jaiswal K, Silva V. (2013) GEM Building Taxonomy (Version 2.0), No. 2013–02. GEM Foundation
- CEN (2004) Eurocode 8: design of structures for earthquake resistance, EN 1998. European Committee for Standardisation, Brussels
- Cornell CA, Jalayer F, Hamburger RO, Foutch DA (2002) Probabilistic basis for 2000 SAC federal emergency management agency steel moment frame guidelines. *J Struct Eng* 128(4):526–533. [https://doi.org/10.1061/\(ASCE\)0733-9445\(2002\)128:4\(526\)](https://doi.org/10.1061/(ASCE)0733-9445(2002)128:4(526))
- da Porto F, Donà M, Rosti A et al (2021) Comparative analysis of the fragility curves for Italian residential masonry and RC buildings. *Bull Earthq Eng* 19:3209–3252. <https://doi.org/10.1007/s10518-021-01120-1>
- De Matteis G, Brando G, Corlito V (2019) Predictive model for seismic vulnerability assessment of churches based on the 2009 L'Aquila earthquake. *Bull Earthq Eng* 17(9):4909–4936. <https://doi.org/10.1007/s10518-019-00656-7>
- Del Gaudio C, Di Ludovico M, Polese M, Manfredi G, Prota A, Ricci P, Verderame GM (2020) Seismic fragility for Italian RC buildings based on damage data of the last 50 years. *Bull Earthq Eng* 18(5):2023–2059. <https://doi.org/10.1007/s10518-019-00762-6>
- Del Gaudio C, Ricci P, Verderame GM (2018) A class-oriented mechanical approach for seismic damage assessment of RC buildings subjected to the 2009 L'Aquila earthquake. *Bull Earthq Eng* 16:4581–4605. <https://doi.org/10.1007/s10518-018-0365-1>
- Del Gaudio C, Ricci P, Verderame GM, Manfredi G (2015) Development and urban-scale application of a simplified method for seismic fragility assessment of RC buildings. *Eng Struct* 91:40–57. <https://doi.org/10.1016/j.engstruct.2015.01.031>
- Del Gaudio C, Ricci P, Verderame GM, Manfredi G (2017) Urban-scale seismic fragility assessment of RC buildings subjected to L'Aquila earthquake. *Soil Dyn Earthq Eng* 96:49–63
- Der Kiureghian A, Ditlevsen O (2008) Aleatory or epistemic? Does it matter? *Struct Saf* 31(2):105–112. <https://doi.org/10.1016/j.strusafe.2008.06.020>
- Di Pasquale G, Orsini G, Romeo RW (2005) New developments in seismic risk assessment in Italy. *Bull Earthq Eng* 3(1):101–128. <https://doi.org/10.1007/s10518-005-0202-1>
- Di Trapani F, Tomaselli G, Cavaleri L, Bertagnoli G (2021) Macroelement model for the progressive-collapse analysis of infilled frames. *J Struct Eng* 147(6):04021079
- DM 17/01/2018 Aggiornamento delle Norme Tecniche per le Costruzioni. *Gazzetta Ufficiale* n. 42. February 20, Rome, 2018 (In Italian)
- Dolce M, Speranza E, Giordano F, Borzi B, Bocchi F, Conte C, Di Meo A, Faravelli M, Pascale V (2019) Observed damage database of past Italian earthquakes: the Da. DO WebGIS. *Bollettino Di Geofisica Teorica Ed Applicata* 60(2):141–164. <https://doi.org/10.4430/bgta0254>
- Donà M, Carpanese P, Follador V, Sbrogì L, da Porto F (2020) Mechanics-based fragility curves for Italian residential URM buildings. *Bull Earthq Eng.* <https://doi.org/10.1007/s10518-020-00928-7>
- Falcone G, Acunzo G, Mendicelli A, Mori F, Naso G, Peronace E, Moscatelli M (2021) Seismic amplification maps of Italy based on site-specific microzonation dataset and one-dimensional numerical approach. *Eng Geol* 289:106170

- FEMA HAZUS99 Technical Manual. (1999) Service Release 2. Federal Emergency Management Agency, Washington, D.C., USA
- Fragiadakis M, Vamvatsikos D, Aschheim M (2014) Application of nonlinear static procedures for the seismic assessment of regular RC moment frame buildings. *Earthq Spectra* 30(2):767–794. <https://doi.org/10.1193/111511EQS281M>
- Galanis PH, Moehle JP (2015) Development of collapse indicators for risk assessment of older-type reinforced concrete buildings. *Earthq Spectra*. <https://doi.org/10.1193/080613EQS225M>
- GNDT Gruppo Nazionale Per la Difesa dai Terremoti, Rischio sismico di edifici pubblici (1993) pp 1–134
- Grünthal G. (1998) European macroseismic scale 1998. European Seismological Commission (ESC)
- Hansapinyo C, Latcharote P, Limkatanyu S (2020) Seismic building damage prediction from GIS-based building data using artificial intelligence system. *Front Built Environ* 6:178. <https://doi.org/10.3389/fbuil.2020.576919>
- Hak S, Morandi P, Magenes G, Sullivan TJ (2012) Damage control for clay masonry infills in the design of RC frame structures. *J Earthq Eng* 16(S1):1–35
- Iervolino I, Galasso C, Cosenza E (2010) REXEL: computer aided record selection for code-based seismic structural analysis. *Bull Earthq Eng* 8(2):339–362
- Indirli M (2019) Organization of a Geographic Information System (GIS) database on natural hazards and structural vulnerability for the historic center of San Giuliano di Puglia (Italy) and the city of Valparaiso (Chile). *Int J Archi Heritage* 3(4):276–315. <https://doi.org/10.1080/15583050902803780>
- ISTAT, 15° Censimento generale della popolazione e delle abitazioni - 9 ottobre 2011, <https://istat.it/>
- Jalayer F, Cornell CA (2009) Alternative non-linear demand estimation methods for probability-based seismic assessments. *Earthq Eng Struct Dyn* 38(8):951–972
- Kazantzi AK, Vamvatsikos D (2015) Intensity measure selection for vulnerability studies of building classes. *Earthq Eng Struct Dyn* 44(15):2677–2694. <https://doi.org/10.1002/eqe.2603>
- Kohrangı M, Bazzurro P, Vamvatsikos D, Spillatura A (2017) Conditional spectrum based ground motion record selection using average spectral acceleration. *Earthq Eng Struct Dyn* 46(10):1667–1685. <https://doi.org/10.1002/eqe.2876>
- Kohrangı M, Bazzurro P, Vamvatsikos D (2021) Seismic risk and loss estimation for the building stock in Isfahan. Part I: Exposure and vulnerability. *Bull Earthq Eng*. <https://doi.org/10.1007/s10518-020-01036-2>
- Kohrangı M, Vamvatsikos (2016) D. INNOSIS ground motion set for medium seismicity European sites http://innoseis.ntua.gr/medium_record_set.rar
- Lachanas CG, Vamvatsikos D (2021) Model type effects on the estimated seismic response of a 20-story steel moment resisting frame. *J Struct Eng* 147(6):04021078. [https://doi.org/10.1061/\(ASCE\)ST.1943-541X.0003010](https://doi.org/10.1061/(ASCE)ST.1943-541X.0003010)
- Lagomarsino S, Giovinazzi S (2006) Macroseismic and mechanical models for the vulnerability and damage assessment of current buildings. *Bull Earthq Eng* 4(4):415–443. <https://doi.org/10.1007/s10518-006-9024-z>
- Leggieri V, Mastrodonato G, Uva G (2022) GIS Multisource data for the seismic vulnerability assessment of buildings at the urban scale. *Buildings* 12(5):523. <https://doi.org/10.3390/buildings12050523>
- Leggieri V, Ruggieri S, Zagari G, Uva G (2021) Appraising seismic vulnerability of masonry aggregates through an automated mechanical-typological approach. *Autom Constr* 132:103972. <https://doi.org/10.1016/j.autcon.2021.103972>
- Liel AB, Haselton CB, Deierlain GG (2011) Seismic collapse safety of reinforced concrete buildings. II: Comparative assessment of nonductile and ductile moment frames. *J Struct Eng* 137(4):492–502. [https://doi.org/10.1061/\(ASCE\)ST.1943-541X.0000275](https://doi.org/10.1061/(ASCE)ST.1943-541X.0000275)
- Lin T, Haselton CB, Baker JW (2013) Conditional spectrum-based ground motion selection. Part I: hazard consistency for risk-based assessments. *Earthq Eng Struct Dyn* 42(12):1847–1865. <https://doi.org/10.1002/eqe.2301>
- McKenna F (2011) OpenSees: a framework for earthquake engineering simulation. *Comput Sci Eng* 13(4):58–66. <https://doi.org/10.1109/MCSE.2011.66>
- Medvedev SV, Spohnauer W, Karnik V (1965) Seismic Intensity Scale Version MSK 1964. Akad. Nauk SSSR, Geofiz. Kom
- Menicelli A, Falcone G, Acunzo G, Mori F, Naso G, Peronace E, Porchia A, Romagnoli G, Moscatelli M (2022) Italian seismic amplification factors for peak ground acceleration and peak ground velocity. *J Maps*. <https://doi.org/10.1080/17445647.2022.2101947>
- Miano A, Jalayer F, Ebrahimian H, Prota A (2018) Cloud to IDA: efficient fragility assessment with limited scaling. *Earthq Eng Struct Dynam* 47(5):1124–1147. <https://doi.org/10.1002/eqe.141>

- Mori F, Mendicelli A, Moscatelli M, Romagnoli G, Peronace E, Naso G (2020) A new Vs30 map for Italy based on the seismic microzonation dataset. *Eng Geol* 275:105745
- Morici M, Canuti C, Dall'Asta A, Leoni G (2020) Empirical predictive model for seismic damage of historical churches. *Bull Earthq Eng* 18(13):6015–6037. <https://doi.org/10.1007/s10518-020-00903-2>
- Mouroux P, Bertrand E, Bour M, Le Brun B, Depinois S, Masure P (2004) The European RISK-UE project: an advanced approach to earthquake risk scenarios. In *Proceedings of the 13th world conference on earthquake engineering*
- Nettis N, Gentile R, Raffaele D, Uva G, Galasso C (2021) Cloud Capacity Spectrum Method: accounting for record-to-record variability in fragility analysis using nonlinear static procedures. *Soil Dyn Earthq Eng*. <https://doi.org/10.1016/j.soildyn.2021.106829>
- Nicodemo G, Pittore M, Masi A, Manfredi V (2020) Modelling exposure and vulnerability from post-earthquake survey data with risk-oriented taxonomies: AeDES form, GEM taxonomy and EMS-98 typologies. *Int J Disaster Risk Reduct* 50:101894. <https://doi.org/10.1016/j.ijdrr.2020.101894>
- Nielson BG, DesRoches R (2007) Seismic fragility methodology for highway bridges using a component level approach. *Earthq Eng Struct Dyn* 36(6):823–839. <https://doi.org/10.1002/eqe.655>
- O'Reilly GJ, Sullivan TJ (2018) Quantification of modelling uncertainty in existing Italian RC frames. *Earthq Eng Struct Dyn* 47(4):1054–1074. <https://doi.org/10.1002/eqe.3005>
- O'Reilly GJ (2021) Limitations of Sa (T1) as an intensity measure when assessing non-ductile infilled RC frame structures. *Bull Earthq Eng* 19(6):2389–2417. <https://doi.org/10.1007/s10518-021-01071-7>
- Panagiotakos TB, Fardis MN. (1996) Seismic response of infilled RC frames structures. In: *11th world conference on earthquake engineering* (No. 225)
- Polese M, Gaetani d'Aragona M, Protà A (2019) Simplified approach for building inventory and seismic damage assessment at the territorial scale: an application for a town in southern Italy. *Soil Dyn Earthq Eng* 121:405–420. <https://doi.org/10.1016/j.soildyn.2019.03.028>
- Polese M, Marcolini M, Zuccaro G et al (2015) Mechanism based assessment of damage-dependent fragility curves for RC building classes. *Bull Earthq Eng* 13:1323–1345. <https://doi.org/10.1007/s10518-014-9663-4>
- Riga E, Karatzetou A, Mara A, Pitilakis K (2017) Studying the uncertainties in the seismic risk assessment at urban scale applying the Capacity Spectrum Method: the case of Thessaloniki. *Soil Dyn Earthq Eng* 92:9–24
- Rosti A, Del Gaudio C, Rota M, Ricci P, Di Ludovico M, Penna A, Verderame GM (2020) Empirical fragility curves for Italian residential RC buildings. *Bull Earthq Eng*. <https://doi.org/10.1007/s10518-020-00971-4>
- Ruggieri S, Cardellicchio A, Leggieri V, Uva G (2021a) Machine-learning based vulnerability analysis of existing buildings. *Autom Constr* 132:103936. <https://doi.org/10.1016/j.autcon.2021.103936>
- Ruggieri S, Perrone D, Leone M, Uva G, Aiello MA (2020a) A prioritization RVS methodology for the seismic risk assessment of RC school buildings. *Int J Disaster Risk Reduct* 51:101807. <https://doi.org/10.1016/j.ijdrr.2020.101807>
- Ruggieri S, Porco F, Fiore A, Raffaele D, Uva G (2019) Influence of infill panels and floor system in the fragility analysis of existing RC buildings: a case study. In: *7th international conference on computational methods in structural dynamics and earthquake engineering, COMPDYN 2019*. <https://doi.org/10.7712/120119.7059.19106>
- Ruggieri S, Porco F, Uva G, Vamvatsikos D (2021b) Two frugal options to assess class fragility and seismic safety for low-rise reinforced concrete school buildings in Southern Italy. *Bull Earthq Eng*. <https://doi.org/10.1007/s10518-020-01033-5>
- Ruggieri S, Tosto C, Perrone D, Uva G, Aiello MA (2021c) Assessment of post-earthquake damages on Italian school building portfolios over the last 50 years. *COMPDYN 2021c, 8th ECCOMAS Thematic Conference on Computational Methods in Structural Dynamics and Earthquake Engineering*. Streamed from Athens, Greece, 27–30 June 2021c
- Ruggieri S, Tosto C, Rosati G, Uva G, Ferro GA (2020b) Seismic vulnerability analysis of Masonry Churches in Piemonte after 2003 Valle Scrivia earthquake: Post-event screening and situation 17 years later. *Int J Arch Heritage*. <https://doi.org/10.1080/15583058.2020.1841366>
- Ruggieri, S. Uva G (2021) Seismic fragility assessment for a class of rc school buildings in italy leveraging detailed and reduced-order models. *COMPDYN 2021*. In: *8th ECCOMAS thematic conference on computational methods in structural dynamics and earthquake engineering*. streamed from Athens, Greece, 27–30 June 2021
- Shinozuka M, Feng MQ, Lee J, Naganuma T (2000) Statistical analysis of fragility curves. *J Eng Mech* 126(12):1224–1231. [https://doi.org/10.1061/\(ASCE\)0733-9399\(2000\)126:12\(1224\)](https://doi.org/10.1061/(ASCE)0733-9399(2000)126:12(1224))
- Silva V, Akkar S, Baker J, Bazzurro P, Castro JM, Crowley H, Dolsek M, Galasso C, Lagomarsino S, Monteiro R, Perrone D, Pitilakis K, Vamvatsikos D (2019) Current challenges and future trends in

- analytical fragility and vulnerability modeling. *Earthq Spectra* 35(4):1927–1952. <https://doi.org/10.1193/042418EQS1010>
- Silva V, Crowley H, Varum H, Pinho R, Sousa L (2014) Investigation of the characteristics of Portuguese regular moment-frame RC buildings and development of a vulnerability model. *Bull Earthq Eng* 13:1–36. <https://doi.org/10.1007/s10518-014-9669-y>
- Smerzini C, Pitolakis K (2018) Seismic risk assessment at urban scale from 3D physics-based numerical modeling: the case of Thessaloniki. *Bull Earthq Eng* 16(7):2609–2631
- Stefanini L, Badini L, Mochi G, Predari G, Ferrante A (2022) Neural networks for the rapid seismic assessment of existing moment-frame RC buildings. *Int J Disaster Risk Reduct* 67:102677. <https://doi.org/10.1016/j.ijdr.2021.102677>
- Uva G, Raffaele D, Porco F, Fiore A (2012) On the role of equivalent strut models in the seismic assessment of infilled RC buildings. *Eng Struct* 42:83–94
- Vamvatsikos D, Cornell CA (2002) Incremental dynamic analysis. *Earthq Eng Struct Dyn* 31(3):491–514
- Vamvatsikos D, Fragiadakis M (2010) Incremental dynamic analysis for estimating seismic performance sensitivity and uncertainty. *Earthq Eng Struct Dyn* 39(2):141–163. <https://doi.org/10.1002/eqe.935>
- Verderame GM, Polese M, Mariniello C, Manfredi G (2010) A simulated design procedure for the assessment of seismic capacity of existing reinforced concrete buildings. *Adv Eng Softw* 41(2):323–335
- Verderame GM, Ricci P, De Risi MT, DeI Gaudio C (2022) Experimental assessment and numerical modeling of conforming and non-conforming RC frames with and without Infills. *J Earth Eng.* <https://doi.org/10.1080/13632469.2019.1692098>
- Vettore M, Donà M, Carpanese P, Follador V, da Porto F, Valluzzi MR (2020) A multilevel procedure at urban scale to assess the vulnerability and the exposure of residential masonry buildings: the case study of Pordenone. *Northeast Italy Heritage* 3(4):1433–1468. <https://doi.org/10.3390/heritage3040080>
- Villar-Vega M, Silva V, Crowley H, Yepes C, Tarque N, Acevedo AB, Hube MA, Gustavo CD, Santa MH (2017) Development of a fragility model for the residential building stock in South America. *Earthq Spectra* 33(2):581–604. <https://doi.org/10.1193/010716EQS005M>
- Vořechovský M, Novák D (2009) Correlation control in small-sample Monte Carlo type simulations I: a simulated annealing approach. *Probab Eng Mech* 24(3):452–462. <https://doi.org/10.1016/j.probenmech.2009.01.004>
- Zanazzi E, Coisson E, Ferretti D (2019) GIS analysis of the seismic damage on historical masonry spires. *International Archives of the Photogrammetry, Remote Sensing Spatial Information Sciences, XLII-2/W11*, 1173–1179. <https://doi.org/10.5194/isprs-archives-XLII-2-W11-1173-2019>
- Zeris C, Vamvatsikos D, Giannitsas P, Alexandropoulos K (2007) Impact of FE modeling in the seismic performance prediction of existing RC buildings. In: *Proceedings of the COMPDYN 2007 conference on computational methods in structural dynamics and earthquake engineering*
- Zuccaro G, Dolce M, De Gregorio D, Speranza E, Moroni C. (2015) La scheda CARTIS per la caratterizzazione tipologico-strutturale dei comparti urbani costituiti da edifici ordinari. *Valutazione dell'esposizione in analisi di rischio sismico. Proceedings of the NINGTS*
- Zucconi M, Romano F, Ferracuti B (2022) Typological fragility curves for RC buildings: influence of damage index and building sample selection. *Eng Struct* 266:114627. <https://doi.org/10.1016/j.engstruct.2022.114627>

Publisher's Note Springer Nature remains neutral with regard to jurisdictional claims in published maps and institutional affiliations.